

Continued functions and critical exponents: Tools for analytical continuation of divergent expressions in phase transition studies

Venkat Abhignan, R. Sankaranarayanan

*Department of Physics, National Institute of Technology, Tiruchirappalli-620015, India.
yvabhignan@gmail.com, sankar@nitt.edu.*

Resummation methods using continued functions are implemented to converge divergent series appearing in perturbation problems related to continuous phase transitions in field theories. In some cases, better convergence properties are obtained using continued functions than diagonal Padé approximants, which are extensively used in literature. We check the reliability of critical exponent estimates derived previously in universality classes of $O(n)$ -symmetric models (classical phase transitions) and Gross-Neveu-Yukawa models (quantum phase transitions) using new methods.

I. INTRODUCTION

Divergent series are inevitable solutions of perturbation approximations used in field theories [1]. Resummation methods are required to extract meaningful values from these perturbative expansions with zero radii of convergence around their singular points [2, 3]. A summation method expands this region of convergence by following a different mapping of variables. The rigorous analysis by Stieltjes on continued fractions has led to the applicability of its analogue Padé sequences on a wide range of problems in perturbation theory [4]. Padé based methods are the most commonly used techniques to achieve these affine transformations of variables by scaling and shifting [5, 6]. Our previous work showed that even other continued functions had remarkably interesting convergence properties by obtaining results related to universal critical parameters [7]. Some important results were discussed, implementing only the lower order information of the renormalization group (RG) perturbative expansions in the $O(n)$ -symmetric ϕ^4 scalar field theory. Especially using the continued exponential [8] and such a blended function, continued exponential fraction, we could address the λ -point discrepancy between the theoretical predictions [9–12], and famous experimental value of specific heat exponent [13] in the $O(2)$ ϕ^4 model [14, 15], though the issue remains unresolved.

Also, using the continued exponential fraction, a consensus can be seen between different theoretical approaches in the most prominently solved three-dimensional Ising model where correlation length exponent $\nu_{Ising} \approx 0.630$ matches up to the third decimal place. The different significant approaches in such models are perturbative RG [16], Monte-Carlo simulations (MC) [17], and conformal bootstrap calculations (CB)[18]. Further, using these continued functions and combining them with Borel-Leroy transformation, we could produce precise estimates for critical parameters in universality classes of modified Landau-Wilson Hamiltonian [19]. Perturbative six-loop ϵ expansions from n -vector model with cubic anisotropy [20], $O(n) \times O(m)$ spin models [21] and the weakly disordered Ising model [22] were handled.

The simplest description for a sequence of the continued functions where the convergent behaviour is observed is that $(i + 1)$ th term of the sequence has the form of i iterations of a corresponding function. Using the self-similar continued representation of a function to obtain convergence was the rudimentary idea developed into many forms by Yukalov [23, 24]. Even the recently developed resummation methods to achieve analytic continuation are based on orthogonal Gauss hypergeometric functions [15, 25–27], which can be represented in the form of continued fractions [28]. However, such methods are based on using the large-order behaviour of the perturbative expansions. Since this asymptotic information might not be available in all cases, it is of prime importance to study resummation methods that only implement lower-order information. For instance, with the recent development in computational techniques, such lower-order information for the ϕ^4 field theory has been solved to calculate the six-loop [29] and seven-loop [16] RG functions. Such calculations involve around 138 Feynman graphs in the fifth order, 687 graphs in the sixth order and 4047 graphs in the seventh order in the perturbative expansions using the minimal subtraction renormalization scheme [29]. With the possibility of solving such complex calculations, it can lead to more orders of information in such field theories, which can better define the behaviour of classical and quantum phase transitions on a wide range of physical systems.

Initially in Sec. II.A we briefly introduce the description of resummation methods. We elaborated and implemented the resummation procedures using continued functions to evaluate divergent expressions concerning the correction-to-scaling exponents derived from the ϕ^4 field theory. Previously we used the continued fraction to solve this series, which can be related to the diagonal Padé approximant in orthogonal polynomials [30–32]. Further in Sec. II.B, we have explored the role of continued exponential in other aspects of continuous phase transitions related to the lattice Ising model. Studying continuous phase transitions on a one-dimensional lattice model with short-range interaction was first proposed by Ising [33]. We implement the continued exponential into the schemes of widely studied perturbative low-temperature expansion [34] and primitive position-space renormalization [35] of the Ising model. Finally, in Sec.III, we explore the possibility of implementing continued functions in the study of critical exponents related to quantum phase transitions using RG functions of Gross-Neveu-Yukawa models [36].

II. CRITICAL EXPONENTS OF CLASSICAL PHASE TRANSITIONS

($O(n)$ UNIVERSALITY CLASS)

A. $O(n)$ -symmetric ϕ^4 field theory and resummation of critical exponents

Studying continuous phase transitions through ϕ^4 field theory begins from Landau's description [37]. The most interesting numerical results that can be derived from implementing Kadanoff's scaling theory [38], Wilson's perturbative RG, and epsilon expansion [39] to this theoretical description of Landau are the critical exponents. They describe the singular behaviour of the phase transition in a material at the critical point $T = T_c$ (critical temperature) and are considered universal, i.e., they are independent of the nature of the material and the type of continuous phase transition. These universal critical parameters are dependent only on the symmetries of the system and dimensionality d , defined by a universality class. These physically relevant yet numerically divergent critical exponents are solved from field theories in the form of

$$Q(\epsilon) \approx \sum_{i=0}^N q_i \epsilon^i \quad (1)$$

for $\epsilon \rightarrow 0$ where ϵ is the perturbative parameter associated with the physical system.

Transformations of sequences is a key numerical technique for resolving convergence issues in the divergent series of critical exponents. The idea behind resummation techniques is that one can achieve convergence by combining the infinite divergent series with an appropriate sequence transformation rather than simply adding a particular series term by term, which is meaningless [2]. A slowly converging or diverging sequence $\{s_N\}_{N=0}^{\infty}$, with the partial sums $\{s_N\} = \sum_{i=0}^N q_i$ of an infinite series, is transformed into a new, presumably better numerically behaved sequence, $\{s'_N\}_{N=0}^{\infty}$ using these resummation methods. Assume that $\{s_N\}_{N=0}^{\infty}$ either converges to a limit s or, if it diverges, can be resummed using the right technique to produce s . Resummation methods implement transformations of linear sequences according to the general formula $s'_N = \sum_{i=0}^N \mu_{Ni} s_i$. These transformations compute the elements of the transformed sequence $\{s'_N\}$ as weighted averages of the elements of the input sequence $\{s_N\}$ with weights μ_{Ni} . The primary argument is that, for the weights μ_{Ni} , it is possible to establish some necessary and sufficient conditions to ensure that, when applied to a convergent sequence $\{s_N\}_{N=0}^{\infty}$, the converted sequence $\{s'_N\}_{N=0}^{\infty}$ may converge to the same limit, $s = s_{\infty}$. Depending on which resummation method is chosen for a specific problem, some empirical ideas are always required to get the best results.

We implement transformation of sequences using continued exponential fraction [7, 19]

$$Q(\epsilon) \sim c_0 \exp \left(\frac{1}{1 + c_1 \epsilon \exp \left(\frac{1}{1 + c_2 \epsilon \exp \left(\frac{1}{1 + c_3 \epsilon \exp \left(\frac{1}{1 + \dots} \right)} \right)} \right)} \right)} \right), \quad (2)$$

continued exponential

$$Q(\epsilon) \sim d_0 \exp(d_1 \epsilon \exp(d_2 \epsilon \exp(d_3 \epsilon \exp(d_4 \epsilon \exp(d_5 \epsilon \exp(d_6 \epsilon \exp(\dots))))))), \quad (3)$$

continued exponential with Borel-Leroy transformation [19]

$$Q(\epsilon) \sim \int_0^{\infty} \exp(-t) t^l e_0 \exp(e_1 \epsilon t \exp(e_2 \epsilon t \exp(e_3 \epsilon t \exp(\dots)))) dt \quad (4)$$

where l is Borel-Leroy parameter, continued natural logarithmic function

$$Q(\epsilon) \sim \log \left(g_1 \epsilon \log \left(g_2 \epsilon \log \left(g_3 \epsilon \log \left(g_4 \epsilon \log \left(g_5 \epsilon \log \left(g_6 \epsilon \log(\dots) + 1 \right) + 1 \right) + 1 \right) + 1 \right) + 1 \right) + 1 \right), \quad (5)$$

and continued fraction

$$Q(\epsilon) \sim \frac{h_0}{\frac{\frac{h_1 \epsilon}{\frac{h_2 \epsilon}{\frac{h_3 \epsilon}{\frac{h_4 \epsilon}{\dots} + 1} + 1} + 1} + 1}}, \quad \text{for } (\epsilon \rightarrow 0). \quad (6)$$

As was previously indicated, Yukalov frequently utilised such continued functions and their combinations for studying convergence [23, 24]. Also, as mentioned earlier, a continued fraction is related to the diagonal Padé approximants and is easily manipulable algebraically [30–32]. Bender and Vinson were the first to investigate continued exponential [8], and

it was later employed for studying convergence in phase transitions [7, 19, 40]. Combining continued exponential and continued fraction, continued exponential fraction was utilised [7]. Continued exponential with Borel-Leroy transformation was utilised based on the Padé-Borel-Leroy transformation

$$Q(\epsilon) = \int_0^\infty \exp(-t)t^l f(\epsilon t) dt, \quad f(y) = \sum_{i=0}^\infty \frac{q_i}{\Gamma(i+l+1)} y^i, \quad (7)$$

replacing Padé with continued exponential [19]. Factorial growth of coefficients q_i can be determined as $i!i!$ similar to $\Gamma(i+l+1)$ in the above equation using Stirling's approximation for large order behaviour ($i \rightarrow \infty$) [3]. The convergence is noted by numerically observing the transformed sequence of calculated quantities

$$C_1 \equiv c_0 \exp\left(\frac{1}{1+c_1\epsilon}\right), \quad C_2 \equiv c_0 \exp\left(\frac{1}{1+c_1\epsilon \exp\left(\frac{1}{1+c_2\epsilon}\right)}\right),$$

$$C_3 \equiv c_0 \exp\left(\frac{1}{1+c_1\epsilon \exp\left(\frac{1}{1+c_2\epsilon \exp\left(\frac{1}{1+c_3\epsilon}\right)}\right)}\right), \dots \quad (8)$$

for continued exponential fraction,

$$D_1 \equiv d_0 \exp(d_1\epsilon), \quad D_2 \equiv d_0 \exp(d_1\epsilon \exp(d_2\epsilon)), \quad D_3 \equiv d_0 \exp(d_1\epsilon \exp(d_2\epsilon \exp(d_3\epsilon))), \dots \quad (9)$$

for continued exponential,

$$E_1 \equiv \int_0^\infty \exp(-t)t^l e_0 \exp(e_1\epsilon t) dt, \quad E_2 \equiv \int_0^\infty \exp(-t)t^l e_0 \exp(e_1\epsilon t \exp(e_2\epsilon t)) dt,$$

$$E_3 \equiv \int_0^\infty \exp(-t)t^l e_0 \exp(e_1\epsilon t \exp(e_2\epsilon t \exp(e_3\epsilon t))) dt, \dots \quad (10)$$

for continued exponential with Borel-Leroy transformation,

$$G_1 \equiv \log(g_1\epsilon + 1), \quad G_2 \equiv \log(g_1\epsilon \log(g_2\epsilon + 1) + 1), \quad G_3 \equiv \log(g_1\epsilon \log(g_2\epsilon \log(g_3\epsilon + 1) + 1) + 1),$$

$$G_4 \equiv \log(g_1\epsilon \log(g_2\epsilon \log(g_3\epsilon \log(g_4\epsilon + 1) + 1) + 1) + 1), \dots \quad (11)$$

for continued logarithm and

$$H_1 \equiv \frac{h_0}{h_1\epsilon + 1}, \quad H_2 \equiv \frac{h_0}{\frac{h_1\epsilon}{h_2\epsilon + 1} + 1}, \quad H_3 \equiv \frac{h_0}{\frac{\frac{h_1\epsilon}{h_2\epsilon + 1}}{h_3\epsilon + 1} + 1}, \quad H_4 \equiv \frac{h_0}{\frac{\frac{\frac{h_1\epsilon}{h_2\epsilon + 1}}{h_3\epsilon + 1}}{h_4\epsilon + 1} + 1}, \dots \quad (12)$$

for continued fraction.

These transformed sequences are calculated for finding a numerical estimate from transformed variables $\{c_i\}$, $\{d_i\}$, $\{e_i\}$, $\{g_i\}$, $\{h_i\}$. These variables can be obtained as general expressions for any quantity $Q(\epsilon)$ by Taylor expansion of sequence at arbitrary order and from relations with coefficients $\{q_i\}$ of Eq.(1) such as (weighted averages of $\{q_i\}$)

$$q_0 = c_0 e^1, \quad q_1 = -c_0 c_1 e^2, \quad q_2 = c_0 e^3 \left(c_1 c_2 + \frac{3c_1^2}{2} \right), \quad q_3 = -c_0 c_1 e^4 \left(\frac{13c_1^2}{6} + 3c_1 c_2 + c_2 c_3 + \frac{3c_2^2}{2} \right), \dots, \quad (13)$$

for continued exponential fraction

$$q_0 = d_0, \quad q_1 = d_0 d_1, \quad q_2 = d_0 \left(d_1 d_2 + \frac{d_1^2}{2} \right), \quad q_3 = d_0 d_1 \left(d_2 d_3 + \frac{d_2^2}{2} + d_1 d_2 + \frac{d_1^2}{6} \right), \dots, \quad (14)$$

for continued exponential

$$q_1 = g_1, \quad q_2 = g_1 g_2, \quad q_3 = g_1 g_2 g_3, \quad q_4 = g_1 g_2 g_3 g_4, \quad q_5 = g_1 g_2 g_3 g_4 g_5, \quad q_6 = g_1 g_2 g_3 g_4 g_5 g_6, \dots, \quad (15)$$

for continued logarithm and

$$q_0 = h_0, \quad q_1 = -h_0 h_1, \quad q_2 = h_0 h_1 (h_2 + h_1), \quad q_3 = -h_0 h_1 (h_2 h_3 + h_2^2 + 2h_1 h_2 + h_1^2), \dots \quad (16)$$

for continued fraction. Solving relations in Eq.(14) for coefficients of Borel-Leroy transformed series $f(y)$ in Eq. (7) provides transformed variables $\{e_i\}$ for continued exponential with Borel-Leroy transformation. While using the continued

logarithmic function, $(g_i \epsilon \log(\dots) + 1) > 0$ condition must be satisfied in every term of the sequence of Eq. (11), or the estimate becomes undefined. And, it is to be noted that this function is applicable only for quantities $Q(\epsilon)$ with $q_0 = 0$. To attain the reliability of the estimates generated by these procedures, error calculation is essential. This is predicted by the principle of fastest apparent convergence, which measures differences of estimates at consecutive orders [29, 41]. The partial sums can be paired with the Shanks transformation for transformed sequences with convergence behaviours to produce accelerated convergence and assess their error [4]. Shanks transformation for a convergent sequence $\{A_i\}$ is defined as

$$S(A_i) = \frac{A_{i+1}A_{i-1} - A_i^2}{A_{i+1} + A_{i-1} - 2A_i}, \quad (17)$$

and iterated Shanks is $S^2(A_i) \equiv S(S(A_i))$. When $S^2(A_i)$ is considered as prediction for $Q(\epsilon)$ the error is estimated from relation [15]

$$(|S(A_{i+1}) - S(A_i)| + |S(A_{i+1}) - S^2(A_i)|)/2. \quad (18)$$

Minimizing this error calculated from successive iterations is also helpful in determining the Borel-Leroy parameter l or tuning parameter in Eq. (7).

1. Critical exponents ν and ω of correlation length ξ

Theoretically, close to the critical point, the correlation length ξ of the fluctuations associated with the field is the most important characteristic length scale. These fluctuations are responsible for the critical behaviour of all the thermodynamic quantities. The divergence of ξ is controlled by the critical exponents ν and ω as

$$\xi(T) \sim |T - T_c|^{-\nu}(1 + \text{const.}|T - T_c|^{\omega\nu} + \dots). \quad (19)$$

For a n -component field, these critical exponents are derived as a power series of $\epsilon = (4 - d)$. In our previous work, continued exponential and continued exponential fraction [7] were used to determine the exponent ν , whereas the recent seven-loop perturbative expansion of ω for $n = 0, 1, 2, 3$ have the form of [15]

$$\omega = \epsilon - 0.65625\epsilon^2 + 1.8236\epsilon^3 - 6.2854\epsilon^4 + 26.873\epsilon^5 - 130.01\epsilon^6 + 692.10\epsilon^7, \quad (20a)$$

$$\omega = \epsilon - 0.62963\epsilon^2 + 1.6182\epsilon^3 - 5.2351\epsilon^4 + 20.750\epsilon^5 - 93.111\epsilon^6 + 458.74\epsilon^7, \quad (20b)$$

$$\omega = \epsilon - 0.60000\epsilon^2 + 1.4372\epsilon^3 - 4.4203\epsilon^4 + 16.374\epsilon^5 - 68.777\epsilon^6 + 316.48\epsilon^7, \quad (20c)$$

$$\omega = \epsilon - 0.57025\epsilon^2 + 1.2829\epsilon^3 - 3.7811\epsilon^4 + 13.182\epsilon^5 - 52.204\epsilon^6 + 226.02\epsilon^7, \quad (20d)$$

for $\epsilon \rightarrow 0$ respectively. Since this series does not have a zeroth order coefficient ($q_0 = 0$), continued exponential and continued exponential fraction could not be directly used to determine a reliable numerical value for exponent ω , and so continued fraction was implemented [7]. Another way of handling this kind of perturbative expansion is perhaps by realizing the series as ω/ϵ (this may not always work correctly for a divergent series [4]). This is used for transformation through continued exponential fraction, continued exponential, continued exponential with Borel-Leroy transformation and continued fraction as defined in Eq.s (2), (3), (4) and (6), respectively. One can directly implement the transformation of ω using continued logarithm as defined in Eq. (5).

In this manner, the numerical estimates of ω for $d = 3$ ($\epsilon = 1$), self-avoiding walks model ($n = 0$) are obtained from sequences $\{C_i\}$, $\{D_i\}$, $\{E_i\}$, $\{G_i\}$, $\{H_i\}$ and their final estimate is interpolated from Shanks in Eq. (17) as

$$C_1 = 0.82327, C_2 = 0.73638, C_3 = 0.77176, C_4 = 0.77159, C_5 = 0.77158, C_6 = 0.77158, S^2(C_4) = 0.77158, \quad (21a)$$

$$D_1 = 0.51879, D_2 = 0.94498, D_3 = 0.62464, D_4 = 0.92862, D_5 = 0.67078, D_6 = 0.92284, S^2(D_4) = 0.665(71), \quad (21b)$$

$$E_1 = 0.55938, E_2 = 0.89477, E_3 = 0.73637, E_4 = 0.84816, E_5 = 0.84818, E_6 = 0.84816, S^2(E_4) = 0.84817, \quad (21c)$$

$$G_2 = -2.6906, G_3 = 0.77963, G_4 = 0.82150, G_5 = 0.84032, G_6 = 0.85018, G_7 = 0.85237, S^2(G_5) = 0.8578(64), \quad (21d)$$

$$H_1 = 0.60377, H_2 = 0.82633, H_3 = 0.76467, H_4 = 0.81070, H_5 = 0.81854, H_6 = 0.80994, S^2(H_4) = 0.8153(33). \quad (21e)$$

These estimates are illustrated in Fig. 1 and compared with the most reliable MC result $\omega = 0.899(12)$ [15, 42]. The error for final estimates is evaluated from Eq. (18). For continued exponential with Borel-Leroy transform, by tuning the parameter l , the plot for a final estimate $S^2(E_4)$ for $l \in [0.5, 2]$ with error bars showing $(|S(E_5) - S(E_4)| + |S(E_5) - S^2(E_4)|)/2$ is illustrated in Fig. 2(a). As it is observed, the final estimate is sensitive to the tuning parameter and taken at $l = 1.43$, where the prediction is most precise with $\omega = 0.84817$. All estimates undershoot, while the continued logarithm estimate $\omega = 0.8578(64)$ is most comparable to the MC value. However, when compared with recent resummation studies, the continued function with Borel-Leroy transform estimate, and continued logarithm estimate are most compatible with previous predictions from hypergeometric-Meijer resummation (HM) [15] (seven-loop) where $\omega = 0.8484(17)$, Borel with conformal mapping calculations (BCM) [29] (six-loop) where $\omega = 0.841(13)$ and self-consistent resummation algorithm (SC) [43] where $\omega = 0.846(15)$. It is also interesting to observe that oscillating sequence from continued exponential envelops the region of convergence from different approaches.

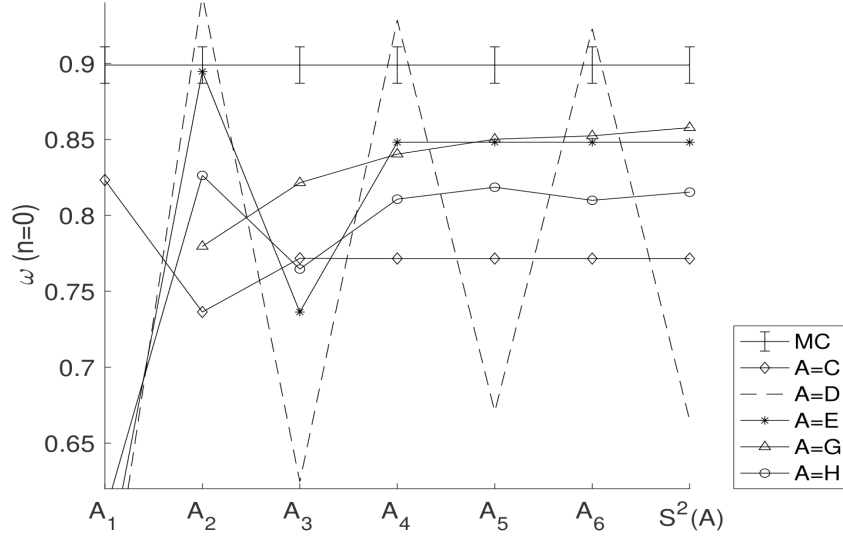


FIG. 1: Estimates of ω at successive orders compared with MC result [15, 42] for self-avoiding walks model.

The numerical estimates of ω for $d = 3$, Ising-like model ($n = 1$) are obtained from sequences

$$C_1 = 0.82856, C_2 = 0.73919, C_3 = 0.77329, C_4 = 0.77278, C_5 = 0.77269, C_6 = 0.77272, S^2(C_4) = 0.77270(2), \quad (22a)$$

$$D_1 = 0.53279, D_2 = 0.93612, D_3 = 0.63803, D_4 = 0.91397, D_5 = 0.68127, D_6 = 0.90431, S^2(D_4) = 0.741(30), \quad (22b)$$

$$E_1 = 0.55458, E_2 = 0.90540, E_3 = 0.70533, E_4 = 0.85741, E_5 = 0.79393, E_6 = 0.82036, S^2(E_4) = 0.81259(2), \quad (22c)$$

$$G_2 = -4.9986, G_3 = 0.75617, G_4 = 0.77396, G_5 = 0.79920, G_6 = 0.80725, G_7 = 0.81013, S^2(G_5) = 0.81174(36), \quad (22d)$$

$$H_1 = 0.61364, H_2 = 0.82364, H_3 = 0.76342, H_4 = 0.80579, H_5 = 0.80533, H_6 = 0.80578, S^2(H_4) = 0.80556(11). \quad (22e)$$

These estimates are illustrated in Fig. 3 and compared with MC result $\omega = 0.832(6)$ [17]. To illustrate the repeatability of behaviour in continued exponential with Borel-Leroy transform, we calculate $S^2(E_4)$ here for varying Borel-Leroy parameter l and plot it in Fig. 2(b). The obtained precise prediction is $\omega = 0.81259(2)$ at $l = 3.53$. This value and continued logarithm estimate $\omega = 0.81174(36)$ are most comparable with the MC result, while other estimates undershoot. The continued logarithm estimate and continued exponential with Borel-Leroy transform estimate are also compatible with recent HM prediction $\omega = 0.82311(50)$, BCM calculation $\omega = 0.820(7)$ and SC algorithm $\omega = 0.827(13)$.

The numerical estimates of ω for $d = 3$, XY universality class ($n = 2$) are obtained from sequences

$$C_1 = 0.83459, C_2 = 0.74368, C_3 = 0.77630, C_4 = 0.77522, C_5 = 0.77475, C_6 = 0.77498, S^2(C_4) = 0.77472(34), \quad (23a)$$

$$D_1 = 0.54881, D_2 = 0.92884, D_3 = 0.65044, D_4 = 0.89975, D_5 = 0.68808, D_6 = 0.88433, S^2(D_4) = 0.774(10), \quad (23b)$$

$$E_1 = 0.58735, E_2 = 0.87944, E_3 = 0.74371, E_4 = 0.81789, E_5 = 0.81785, E_6 = 0.74371, S^2(E_4) = 0.81789(2), \quad (23c)$$

$$G_2 = -2.4804, G_3 = 0.73100, G_4 = 0.72010, G_5 = 0.75477, G_6 = 0.75999, G_7 = 0.76383, S^2(G_5) = 0.81174(36), \quad (23d)$$

$$H_1 = 0.62500, H_2 = 0.82329, H_3 = 0.76388, H_4 = 0.80231, H_5 = 0.79408, H_6 = 0.80029, S^2(H_4) = 0.7983(14). \quad (23e)$$

These estimates are illustrated in Fig. 4 and compared with MC result $\omega = 0.789(4)$ [12]. The continued fraction estimate $\omega = 0.7983(14)$ is most comparable with the MC value, while other estimates undershoot or overshoot. The continued function with Borel-Leroy transform estimate $\omega = 0.81789$ ($l = 1.26$) and continued logarithm estimate $\omega = 0.81174(36)$ is most compatible with CB result $\omega = 0.811(10)$ [44], HM prediction $\omega = 0.789(13)$ and BCM calculation $\omega = 0.804(3)$.

The numerical estimate of ω for $d = 3$, Heisenberg universality class ($n = 3$) are obtained from sequences

$$C_1 = 0.84080, C_2 = 0.74909, C_3 = 0.78036, C_4 = 0.77855, C_5 = 0.77572, C_6 = 0.77784, S^2(C_4) = 0.7807(52), \quad (24a)$$

$$D_1 = 0.56538, D_2 = 0.92316, D_3 = 0.66270, D_4 = 0.88691, D_5 = 0.69486, D_6 = 0.86466, S^2(D_4) = 0.7831(17), \quad (24b)$$

$$E_1 = 0.60287, E_2 = 0.87481, E_3 = 0.74859, E_4 = 0.80427, E_5 = 0.804425, E_6 = 0.80427, S^2(E_4) = 0.80435(4), \quad (24c)$$

$$G_2 = -1.8614, G_3 = 0.70588, G_4 = 0.66200, G_5 = 0.70910, G_6 = 0.71041, G_7 = 0.71550, S^2(G_5) = 0.70877(96), \quad (24d)$$

$$H_1 = 0.63684, H_2 = 0.82452, H_3 = 0.76614, H_4 = 0.80025, H_5 = 0.78725, H_6 = 0.79218, S^2(H_4) = 0.79083. \quad (24e)$$

These estimates are illustrated in Fig. 5 and compared with MC result $\omega = 0.773$ [45]. The continued exponential estimate $\omega = 0.7831(17)$, continued exponential fraction estimate $\omega = 0.7807(52)$ are comparable with the MC value and similarly continued fraction estimate $\omega = 0.79083$, continued exponential with Borel-Leroy transform estimate $\omega = 0.80435(4)$ ($l = 1.16$) are most compatible with predictions from BCM calculation $\omega = 0.795(7)$ and SC resummation algorithm $\omega = 0.794(4)$.

Similarly, we study ω for $d = 2$ ($\epsilon = 2$) systems. These results are interesting since previous resummation studies of RG functions could not predict reliable estimates for two-dimensional systems [46–48] due to non-analyticity of β -functions around the fixed point. We obtain numerical estimates of ω for $d = 2$ self-avoiding walks model (Eq. (20a)) from the

sequences at consecutive orders as

$$C_1 = 1.4442, C_2 = 1.3059, C_3 = 1.3685, C_4 = 1.3682, C_5 = 1.3682, C_6 = 1.3682, S^2(C_4) = 1.3682, \quad (25a)$$

$$D_1 = 0.53829, D_2 = 1.9806, D_3 = 0.60286, D_4 = 1.9793, D_5 = 0.61259, D_6 = 1.9792, S^2(D_4) = 1.276(11), \quad (25b)$$

$$E_1 = 0.68393, E_2 = 1.8792, E_3 = 1.0471, E_4 = 1.7958, E_5 = 1.7542, E_6 = 1.0583, S^2(E_4) = 1.805(24), \quad (25c)$$

$$G_2 = 1.8597, G_3 = 1.6694, G_4 = 1.8057, G_5 = 1.8065, G_6 = 1.8152, G_7 = 1.8154, S^2(G_5) = 1.8064(93), \quad (25d)$$

$$H_1 = 0.86486, H_2 = 1.5997, H_3 = 1.3194, H_4 = 1.5533, H_5 = 1.6082, H_6 = 1.5509, S^2(H_4) = 1.589(27). \quad (25e)$$

These estimates are illustrated in Fig. 6 and compared with exact result from lattice models, $\omega = 2$ [49, 50]. Continued with Borel-Leroy transform estimate $\omega = 1.805(24)$ ($l = 1.75$), continued logarithm estimate $\omega = 1.8064(93)$ are comparable with the exact result, HM resummation $\omega = 1.96(46)$ and BCM prediction $\omega = 1.90(25)$.

We obtain numerical estimates of ω for $d = 2$ Ising-like model from the sequences as

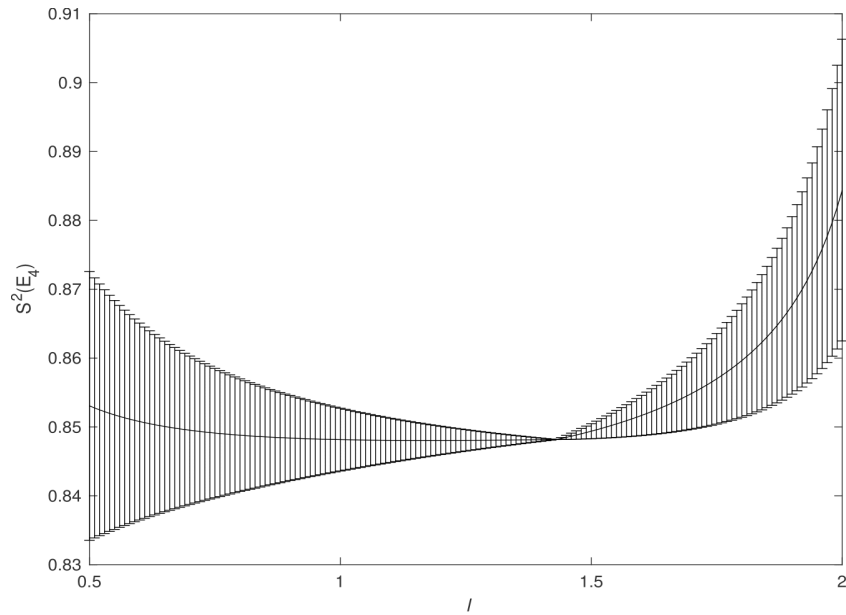
$$C_1 = 1.4573, C_2 = 1.3113, C_3 = 1.3725, C_4 = 1.3717, C_5 = 1.3716, C_6 = 1.3716, S^2(C_4) = 1.3716(1), \quad (26a)$$

$$D_1 = 0.56773, D_2 = 1.9725, D_3 = 0.64065, D_4 = 1.9696, D_5 = 0.65243, D_6 = 1.9693, S^2(D_4) = 1.2981(78), \quad (26b)$$

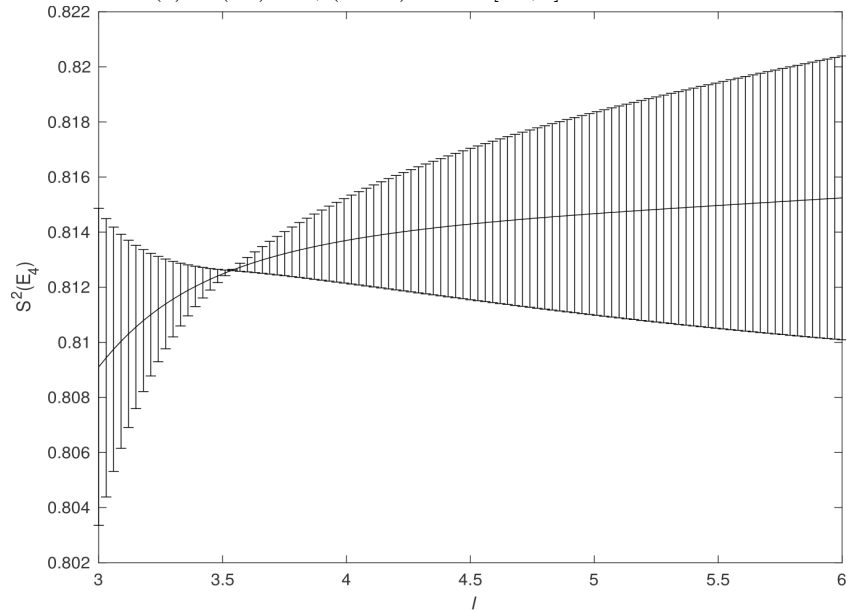
$$E_1 = 0.72905, E_2 = 1.8469, E_3 = 1.1097, E_4 = 1.7273, E_5 = 1.7283, E_6 = 1.7273, S^2(E_4) = 1.7278(3), \quad (26c)$$

$$G_2 = 1.8732, G_3 = 1.6453, G_4 = 1.7843, G_5 = 1.7842, G_6 = 1.7936, G_7 = 1.7938, S^2(G_5) = 1.7842(95), \quad (26d)$$

$$H_1 = 0.88525, H_2 = 1.5898, H_3 = 1.3127, H_4 = 1.5348, H_5 = 1.5316, H_6 = 1.5348, S^2(H_4) = 1.5333(8). \quad (26e)$$



(a) $S^2(E_4)$ vs l , ($n = 0$) for $l \in [0.5, 2]$.



(b) $S^2(E_4)$ vs l , ($n = 1$) for $l \in [3, 6]$.

FIG. 2: The estimate of ω derived from $S^2(E_4)$ vs shift parameter l is plotted, with the error bars showing the value of $(|S(E_5) - S(E_4)| + |S(E_5) - S^2(E_4)|)/2$.

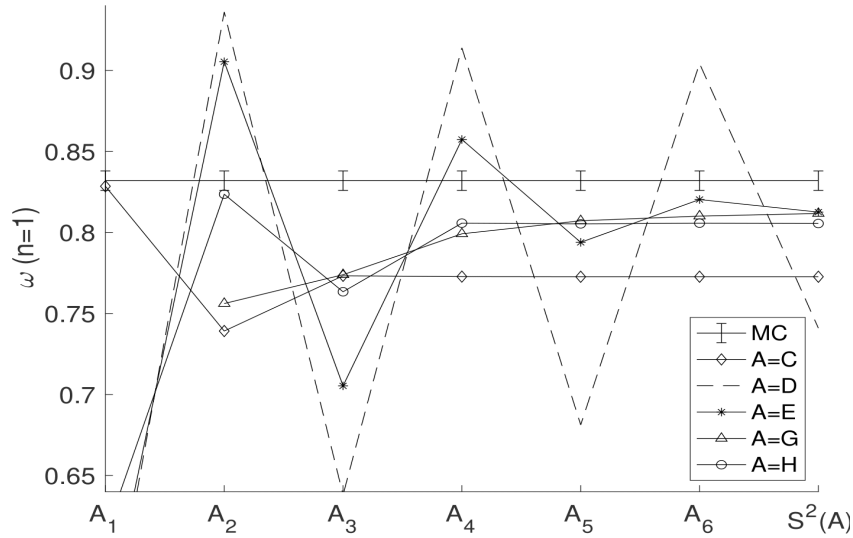


FIG. 3: Estimates of ω at successive orders compared with MC result [17] for Ising-like model.

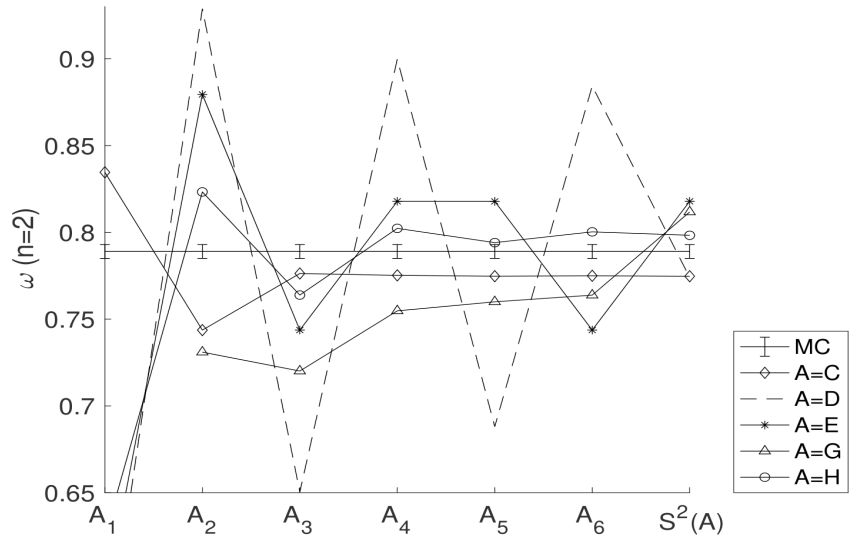


FIG. 4: Estimates of ω at successive orders compared with MC result [12] for XY universality class.

These estimates are illustrated in Fig. 7 and compared with the exact result from the lattice model, $\omega = 1.75$ [48]. For this model, the estimate from continued exponential with Borel-Leroy transform $\omega = 1.7278(3)$ ($l = 1.36$) and continued logarithm estimate $\omega = 1.7842(95)$ are compatible with the exact value. Similarly, the HM prediction $\omega = 1.71(10)$ and BCM calculation $\omega = 1.71(9)$ for the Ising-like model illustrate that resummation of ϵ -expansions gives better estimates than the resummation of the coupling-series [3]. It is noted here that while procedures such as BCM and HM implement, large-order asymptotic information of RG functions, our methods implement only the lower-order information as described. Other exponents related to scaling exponent ν can be approximately estimated from the Gaussian model (mean-field theory). In contrast, the measurement of subleading exponent ω completely requires the corrections from perturbative RG and is important to understand the relevant directions in RG flows. Hence the procedures where only the corrections are used without external parameters to measure the exponent ω are more reliable.

A more stringent check for these procedures would be to obtain the most accurately measured result from the microgravity experiment for superfluid helium where specific heat exponent $\alpha_{XY} = -0.0127(3)$ [13]. Using the slowly converging seven-loop ϵ expansion [15] of

$$\nu_{XY} = 2.0000 - 0.40000\epsilon - 0.14000\epsilon^2 + 0.12244\epsilon^3 - 0.30473\epsilon^4 + 0.87924\epsilon^5 - 3.1030\epsilon^6 + 12.419\epsilon^7, \quad (27)$$

we obtain the sequences directly for continued exponential fraction, continued exponential, continued exponential with

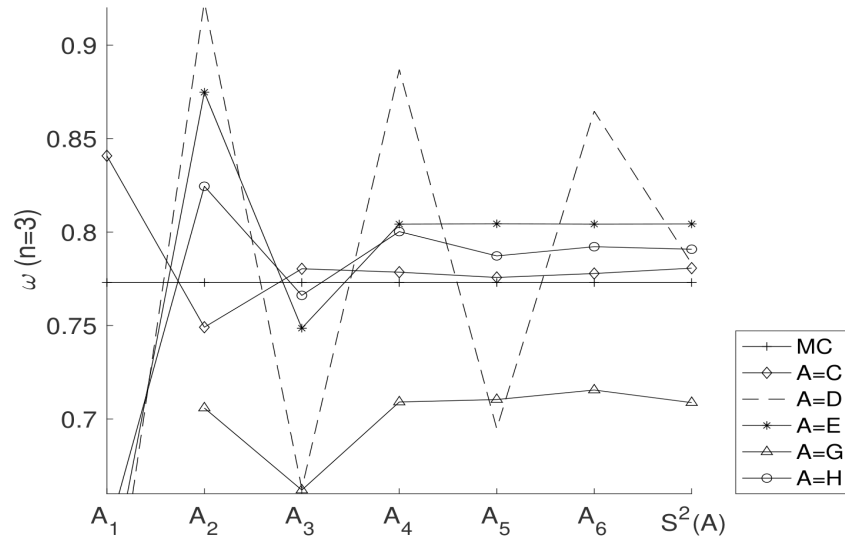


FIG. 5: Estimates of ω at successive orders compared with MC result [45] for Heisenberg universality class.

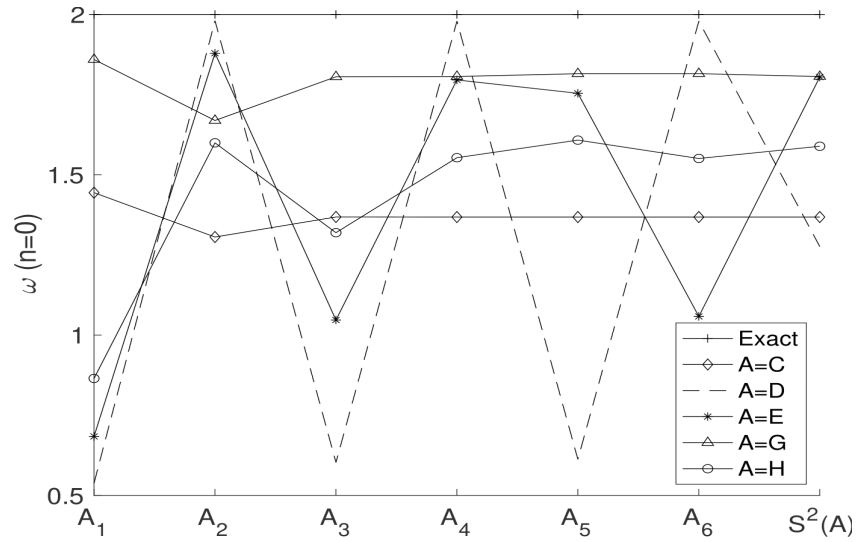


FIG. 6: Estimates of ω at successive orders for self-avoiding walks model compared with exact result [49, 50] in two-dimensional system.

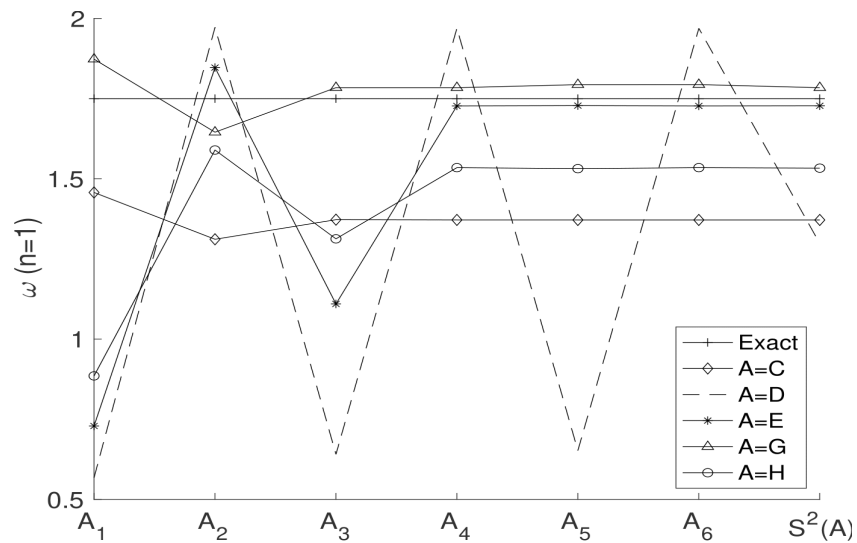


FIG. 7: Estimates of ω at successive orders for Ising-like model compared with exact result [48] in two dimensional system.

Borel-Leroy transform, continued fraction and estimates for ν_{XY} in $d = 3$ at consecutive orders as

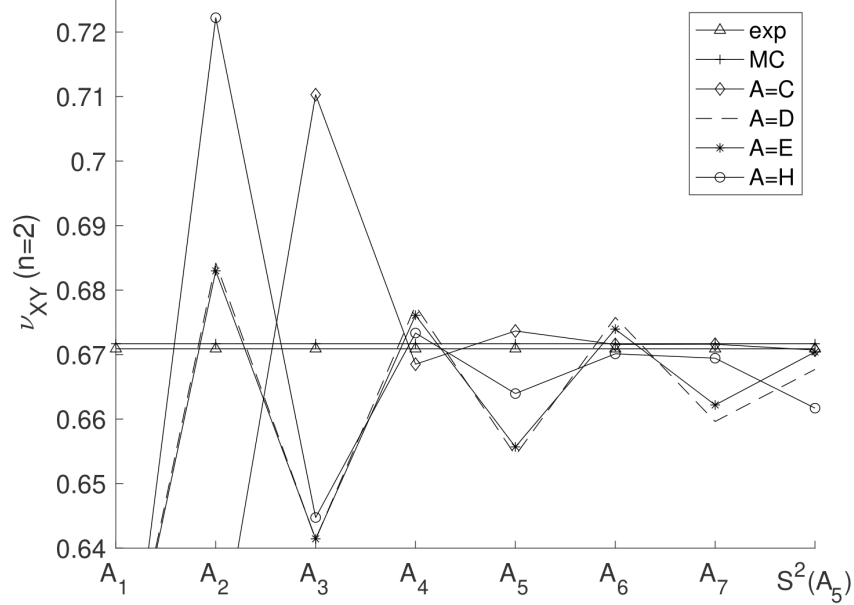
$$C_1 = 0.53547, C_2 = 0.61992, C_3 = 0.71029, C_4 = 0.66851, C_5 = 0.67366, C_6 = 0.67157, C_7 = 0.67161, \\ S^2(C_5) = 0.67070(74), \quad (28a)$$

$$D_1 = 0.61070, D_2 = 0.68421, D_3 = 0.64135, D_4 = 0.67758, D_5 = 0.65436, D_6 = 0.67576, D_7 = 0.65963, \\ S^2(D_5) = 0.6677(11), \quad (28b)$$

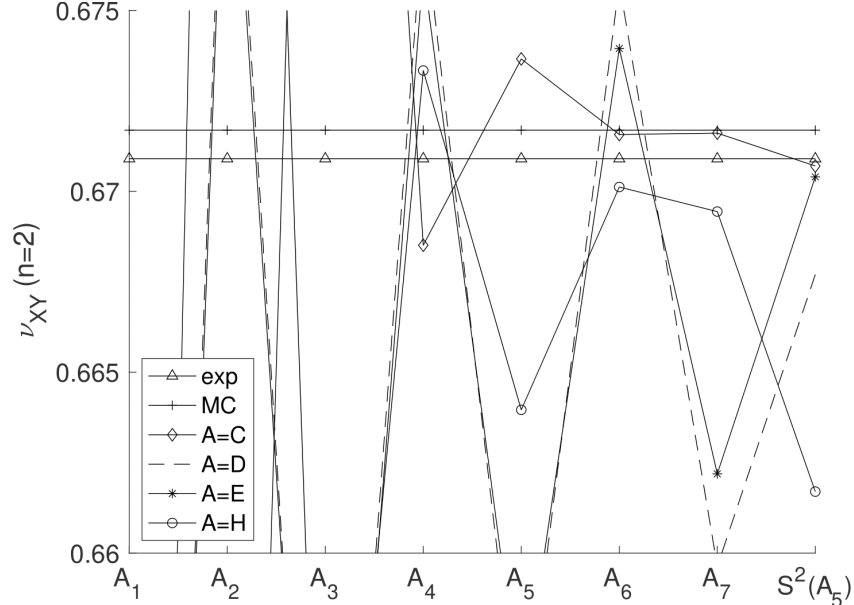
$$E_1 = 0.61018, E_2 = 0.68298, E_3 = 0.64144, E_4 = 0.67610, E_5 = 0.65569, E_6 = 0.67395, E_7 = 0.66219, \\ S^2(D_5) = 0.6704(25), \quad (28c)$$

$$H_1 = 0.60000, H_2 = 0.72222, H_3 = 0.64474, H_4 = 0.67334, H_5 = 0.66396, H_6 = 0.67012, H_7 = 0.66944, \\ S^2(H_5) = 0.6617(48). \quad (28d)$$

We compare these estimates with microgravity experimental value (exp) $\nu_{XY} = 0.6709(1)$ [13] and most reliable MC result $\nu_{XY} = 0.67169(7)$ [12] in Fig. 8. The oscillating sequences converging towards these precise values can be visualized in



(a) Oscillating convergence of ν_{XY} from continued functions.



(b) Seven-loop resummation of ν_{XY} .

FIG. 8: The estimates of ν_{XY} compared with precise experimental value [13] and MC result [12].

Fig. 8(a). Using the continued exponential with Borel-Leroy transform, we obtain the estimate $\nu_{XY} = 0.6704(25)$ at $l = 22.51$ (Fig. 9), where it is observed that $\nu_{XY} \in [0.669, 0.677]$ for $l \in [10, 25]$.

Further using Josephson's identity, $\alpha = 2 - d\nu$, we obtain estimates for continued exponential fraction, continued exponential, continued exponential with Borel-Leroy transform and continued fraction as $\alpha_{XY} = -0.0121(22)$, $\alpha_{XY} = -0.017(20)$, $\alpha_{XY} = -0.0112(76)$ and $\alpha_{XY} = 0.015(14)$, respectively. The initial three estimates and recent resummation of seven-loop RG $\alpha_{XY} = -0.0123(11)$ (HM) seem more compatible with the precise experimental value. However, the

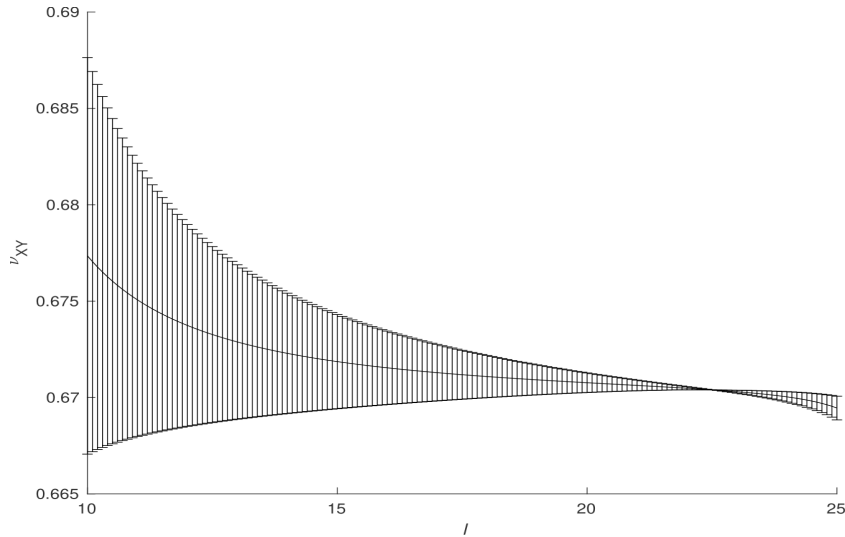


FIG. 9: The estimate of ν_{XY} vs shift parameter l is plotted, with the error bars showing the relation for error.

significant errors in these predictions from RG are concerning since they cannot completely address the mismatch of predictions from MC and experimental value [14] which can be distinctly seen in Fig. 8(b). Eight-loop RG functions may help in resolving these issues.

B. Lattice Ising model ($n = 1$)

Considering the microscopic degrees of freedom, the discrete lattice Ising model provides the same statistical description to describe the nature of continuous phase transitions in $O(1)$ ϕ^4 field models. The partition function of the simplest one-dimensional Ising model [51] is,

$$Z = \sum_{\{\sigma_i\}} \exp \left[\sum_{\langle i,j \rangle} B(\sigma_i, \sigma_j) \right] = \sum_{\{\sigma_i\}} \exp \left[K \sum_{\langle i,j \rangle} \sigma_i \sigma_j + \frac{h}{2} \sum_{\langle i,j \rangle} (\sigma_i + \sigma_j) \right]. \quad (29)$$

where $\sigma_i = \pm 1$ is the spin at each lattice site i . $B(\sigma_i, \sigma_j)$ is the energy per bond between two nearest neighbour lattice sites i and j . Here $K = J/k_B T$, J is the nearest neighbour coupling constant, and h is the external magnetic field. The partition function just over the nearest neighbours is taken as

$$Z = \sum_{\{\sigma_i\}} \exp \left[\sum_{\langle i,i+1 \rangle} B(\sigma_i, \sigma_{i+1}) \right]. \quad (30)$$

$\sum_{\{\sigma_i\}}^{N'}$ indicates summing over all possible $2^{N'}$ configurations of N' spins and $\sum_{\langle i,i+1 \rangle}$ indicates summation over all nearest neighbour pairs. Though no phase transition exists on this one-dimensional model, extension to two dimensions led to interesting analytical conclusions based on Kramers-Wannier duality [52] in the seminal work by Onsager [53]. This is used to study ordering in paramagnetic-ferromagnetic transitions.

1. Low temperature expansions

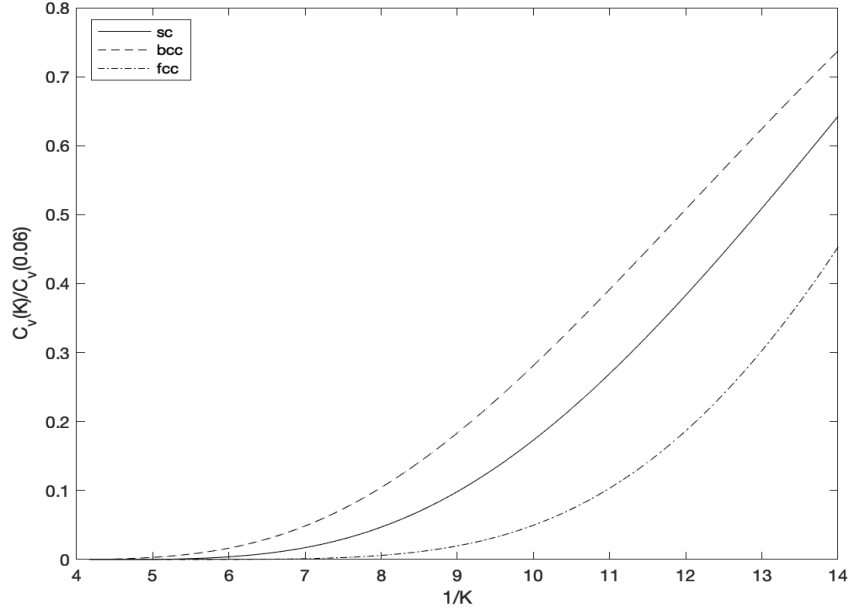
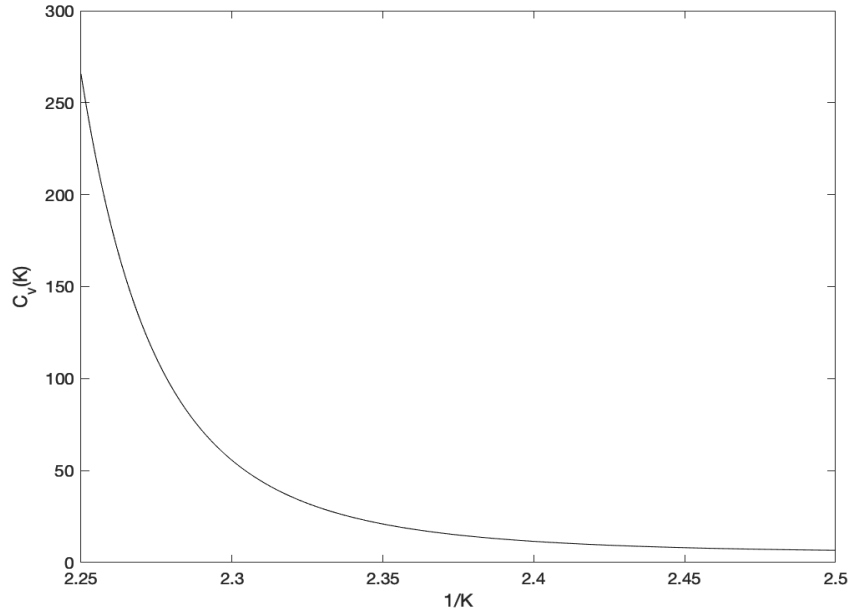
Different perspectives are used for solving this partition function Z of two and three-dimensional Ising models [34]. A diagrammatic approach was used to capture the co-existence of different phases in the vicinity of critical points using the method of low-temperature expansions. The partition function Z was derived by studying excitation and interactions among the excitation around the most stable configuration at $T \rightarrow 0$. These series expansions are divergent, and so initially, Padé approximants were applied by Baker to obtain an analytic continuation [54, 55]. Similarly, we use continued exponential to study the extensive quantity, specific heat C_v derived from such low-temperature expansions in the factors of $u = \exp(-4K)$. The critical exponent α can be derived by studying the behaviour of C_v at constant volume near the critical temperature as $C_v \sim |T - T_c|^{-\alpha}$.

Here we study the behaviour of $C_v(K)$ [54] close to the critical point K_c ($\sim 1/T_c$) for the $d = 2$ simple quadratic lattice (sq) where

$$C_v(K)/K^2 = 64u^2 + 288u^3 + 1152u^4 + 4800u^5 + 21504u^6 + 101920u^7 + 502016u^8 + 2538432u^9 + 13078720u^{10} + 68344496u^{11}, \quad (31)$$

$d = 3$ simple cubic lattice (sc) where

$$C_v(K)/K^2 = 144u^3 + 1200u^5 - 2016u^6 + 11760u^7 - 33792u^8 + 135216u^9 - 448800u^{10} + 1643664u^{11} - 5671872^{12}, \quad (32)$$

(a) Comparing C_v vs $1/K$ values for sc, bcc and fcc.(b) C_v vs $1/K$ values for sq.FIG. 10: Illustrating the behaviour of C_v vs $1/K$ for $d = 3$ and $d = 2$ lattice around $1/K_c$.

$d = 3$ body-centred cubic lattice (bcc) where

$$C_v(K)/K^2 = 256u^4 + 3136u^7 - 4608u^8 + 4480u^{10} - 123904u^{11} + 111360u^{12} + 551616u^{13} - 2464896u^{14} + 4190400u^{15}, \quad (33)$$

and $d = 3$ face-centered cubic lattice (fcc) where

$$C_v(K)/K^2 = 576u^6 + 11616u^{11} - 14976u^{12} + 28800u^{15} + 172032u^{16} - 554880u^{17} + 374976u^{18} + 138624u^{19} + 787200u^{20}. \quad (34)$$

The Taylor expressions around $K = 0$ for these expressions of $C_v(K)/K^2$ are recast into continued exponential (Eq. (3)) up to the ninth order such as

$$\text{sq: } 84593392 \exp(-43.044K \exp(-0.0557K \exp(2.0512K \exp(0.9789K \exp(1.0873K \exp(1.1605K \exp(0.8735K \exp(0.2115K \exp(-9.9314K)))))))))) \quad (35)$$

$$\text{sc: } -54793248 \exp(-56.9186K \exp(0.0277K \exp(1.3411K \exp(2.2139K \exp(4.3708K \exp(1.5199K \exp(0.069K \exp(-57.104K \exp(34.032K)))))))))) \quad (36)$$

$$\text{bcc: } -34418496 \exp(-68.824K \exp(0.03089K \exp(2.0647K \exp(2.7629K \exp(5.6212K \exp(1.9136K \exp(-0.6834K \exp(14.292K \exp(-1.2633K)))))))))) \quad (37)$$

$$\text{fcc: } 4366089 \exp(-96.531K \exp(0.2539K \exp(1.1231K \exp(-11.0745K \exp(25.0895K \exp(6.7036K \exp(13.5554K \exp(6.4608K \exp(15.9134K)))))))))) \quad (38)$$

assuming that low-temperature expansions around $K = 0$ are sufficient to capture the nature of singular behaviour. To illustrate the behaviour of expressions of the continued exponential, we plot $C_v(K)/C_v(0.06)$ around the critical points $1/K_c$ for $d = 3$ sc, bcc and fcc in Fig. 10(a). The $C_v(K)$ is normalised with an arbitrarily high value $C_v(0.06)$, and it can be observed that this captures a similar singular nature for sc, bcc and fcc in the vicinity of $1/K_c$ from the low-temperature side. The critical values for $1/K_c$ in the literature [54] are given by $1/0.4407 = 2.2692$, $1/0.2217 = 4.5102$, $1/0.1575 = 6.3505$, $1/0.1021 = 9.7923$ for sq, sc, bcc and fcc correspondingly. Similarly, $C_v(K)$ for $d = 2$ sq seems to possess singular nature from the high-temperature side in Fig. 10(b). This unique behaviour may be related to the Kramers-Wannier duality on square lattice [52] where the strong coupling at low temperature gets mapped to the weak coupling at high temperature and vice-versa. From these curves, it is deduced that the value for exponent α at their corresponding K_c is $\alpha = 0.1026, 0.1193$ for three-dimensional bcc, fcc and $\alpha = -0.0138$ for two-dimensional sq respectively. These seem to be comparable with values $\alpha = 0.11$ for $d = 3$ and $\alpha = 0$ for $d = 2$ Ising models [51].

2. Migdall-Kadanoff position space renormalization

Kadanoff's renormalization scheme was used on two-dimensional Ising models using successive approximations to control the divergent long-range interactions, and the correlation length critical exponent $\nu_{Ising} \approx 1$ was extracted [35, 56, 57]. However, the primitive renormalization approach [35] does not produce a reliable estimate of ν_{Ising} , which was systematically improved later [56, 57]. Similarly, we take the most straightforward position space renormalization scheme of the one-dimensional Ising model, where the decimation of every alternate spin on the lattice essentially reduces the N' degrees of freedom by a rescaling factor of $b = 2$ in Eq.(30) [51]. Then we introduce new interactions in the renormalization scheme to account for long-range behaviour and implement continued exponential to approximate the divergent interactions controlled by a free parameter a . Further, Migdal-Kadanoff bond moving approximation is used to obtain exponent ν_{Ising} for phase transitions on fractal systems with non-integer dimensions $1 < d < 2$.

There is a simple mapping between the original spins to the renormalized spins ($\{\sigma_i\} \mapsto \{\sigma'_i\}$) in the partition function Z (Eq. 30) after summing over the decimated spins s_i as [51]

$$\sum_{\{\sigma'_i\}} \sum_{\{s_i\}} \exp \left[\sum_{i=1}^{N'/2} B(\sigma'_i, s_i) + B(s_i, \sigma'_{i+1}) \right] = \sum_{\{\sigma'_i\}} \prod_{i=1}^{N'/2} \left[\sum_{s_i=\pm 1} e^{B(\sigma'_i, s_i) + B(s_i, \sigma'_{i+1})} \right] \equiv \sum_{\{\sigma'_i\}} e^{\left[\sum_{\langle i, i+1 \rangle} B'(\sigma'_i, \sigma'_{i+1}) \right]}. \quad (39)$$

Where the bond energy of the renormalized spins is

$$B'(\sigma'_1, \sigma'_2) = \frac{h'}{2}(\sigma'_1 + \sigma'_2) + K' \sigma'_1 \sigma'_2. \quad (40)$$

The renormalized interactions are obtained from the assumption that the renormalized parameters (h', K') are functions of (h, K) having similar formalism. We assume here that the renormalized parameters (h', K') are analytical functions of (h, K) since it reflects Kadanoff's scaling idea [38]. h and K are independent parameters that govern the continuous phase transition in a ferromagnetic-paramagnetic system around the point of criticality. The renormalized Hamiltonian per bond with the renormalized interactions is

$$\begin{aligned} R(\sigma'_1, \sigma'_2) &\equiv \exp \left[K' \sigma'_1 \sigma'_2 + \frac{h'}{2}(\sigma'_1 + \sigma'_2) \right] \\ &= \sum_{s_1=\pm 1} \exp \left[k_1(K\sigma'_1 s_1 + K\sigma'_2 s_1 + K_2(\sigma'_1 s_1)(\sigma'_2 s_1)) + h_1 \left(\frac{h}{2}(\sigma'_1 + s_1) + \frac{h}{2}(\sigma'_2 + s_1) \right) + \right. \\ &\quad k_2((K\sigma'_1 s_1)^2 + (K\sigma'_2 s_1)^2 + K_2^2(\sigma'_1 s_1)^2(\sigma'_2 s_1)^2) + \\ &\quad h_2 \left(\left(\frac{h}{2}\sigma'_1 \right)^2 + \left(\frac{h}{2}\sigma'_2 \right)^2 + 2 \left(\frac{h}{2}s_1 \right)^2 \right) + \\ &\quad k_3((K\sigma'_1 s_1)^3 + (K\sigma'_2 s_1)^3 + K_2^3(\sigma'_1 s_1)^3(\sigma'_2 s_1)^3) + \\ &\quad \left. h_3 \left(\left(\frac{h}{2}\sigma'_1 \right)^3 + \left(\frac{h}{2}\sigma'_2 \right)^3 + 2 \left(\frac{h}{2}s_1 \right)^3 \right) + \dots \right], \quad (41) \end{aligned}$$

where $\{k_i\}$ and $\{h_i\}$ are the coefficients associated with the power series. The above expression $R(\sigma'_1, \sigma'_2)$ is the most generalized series expansion. Though it reduces the degrees of freedom, the renormalisation procedure typically introduces more interactions than in the original Hamiltonian. We introduce a new long-range interaction due to the renormalization procedure between pair of spin pairs $(\sigma'_1 s_1)$ and $(\sigma'_2 s_1)$ with a probabilistic weight K_2 in the probabilistic description.

Since $\sigma_i^2, s_1^2 = 1$ and $\sigma_i^3 = \sigma_i', s_1^3 = s_1$, the probabilistic weight is not going to change due to them. So we do not include the power series terms of the individual spins and spin pairs for determining the renormalized interactions. Rather, we include only the terms with K_2 assigning the weight $K_2 = K^a$. We assign a as the parameter that controls the strength of long-range interactions. To confine the long-range interactions, we convert the analytical function to a continued exponential such that $k_i = (i+1)^{i-1}/i!$ and renormalized interactions $R(\sigma_1', \sigma_2')$ becomes

$$R(\sigma_1', \sigma_2') = \exp \left[K' \sigma_1' \sigma_2' + \frac{h'}{2} (\sigma_1' + \sigma_2') \right] = e^{K^a \sigma_1' \sigma_2' e^{K^a \sigma_1' \sigma_2' e^{K^a \sigma_1' \sigma_2' e^{\dots}}}} \sum_{s_1 = \pm 1} \exp \left[K \sigma_1' s_1 + K \sigma_2' s_1 + \frac{h}{2} (\sigma_1' + \sigma_2') + h s_1 \right]. \quad (42)$$

All the possible configurations of the spins are considered,

$$\begin{aligned} R(+1, +1) &= e^{K'} e^{h'} = e^{K^a e^{K^a e^{K^a e^{\dots}}}} e^h (e^{2K} e^h + e^{-2K} e^{-h}), \\ R(-1, -1) &= e^{K'} e^{-h'} = e^{K^a e^{K^a e^{K^a e^{\dots}}}} e^{-h} (e^{-2K} e^h + e^{2K} e^{-h}), \\ R(+1, -1) &= e^{-K'} = e^{-K^a e^{-K^a e^{-K^a e^{\dots}}}} (e^h + e^{-h}), \\ R(-1, +1) &= e^{-K'} = e^{-K^a e^{-K^a e^{-K^a e^{\dots}}}} (e^h + e^{-h}). \end{aligned}$$

The solutions for the above take the form of

$$e^{4K'} = \frac{e^{2K^a e^{K^a e^{K^a e^{\dots}}}} (e^{2K} e^h + e^{-2K} e^{-h}) (e^{-2K} e^h + e^{2K} e^{-h})}{e^{-2K^a e^{-K^a e^{-K^a e^{\dots}}}} (e^h + e^{-h})^2}, \quad (43)$$

$$e^{2h'} = \frac{e^{2h} (e^{2K} e^h + e^{-2K} e^{-h})}{(e^{-2K} e^h + e^{2K} e^{-h})}. \quad (44)$$

The critical point K_c can be found by setting $h = 0$ since its a symmetry-breaking term, so studying the characteristics of K in a subspace where the symmetry is maintained such that $h = 0$ implies $h' = 0$,

$$e^{2K'} = \frac{e^{K^a e^{K^a e^{K^a e^{\dots}}}} (e^{-2K} + e^{2K})}{2e^{-K^a e^{-K^a e^{-K^a e^{\dots}}}}}. \quad (45)$$

We obtain the fixed point for the above recursion relation of K such that the sequence

$$\frac{1}{2} \ln \left(\frac{e^{K_c^a} (e^{-2K_c} + e^{2K_c})}{2e^{-K_c^a}} \right), \frac{1}{2} \ln \left(\frac{e^{K_c^a e^{K_c^a}} (e^{-2K_c} + e^{2K_c})}{2e^{-K_c^a e^{-K_c^a}}} \right), \frac{1}{2} \ln \left(\frac{e^{K_c^a e^{K_c^a e^{K_c^a}}} (e^{-2K_c} + e^{2K_c})}{2e^{-K_c^a e^{-K_c^a e^{-K_c^a}}}} \right), \dots \quad (46)$$

approaches a converged value of K_c , the point of criticality where we are interested in studying the interactions. For $d > 1$ where the ordering happens, we use the Migdall-Kadanoff bond moving approximation where the bond strengthens by a factor 2^{d-1} (K becomes $2^{d-1}K$) for any d -dimensional hypercubic lattice in Eq.(43). Using this formalism, we get $K_c = 0.1271$ for $d = 2$ taking $a = 2$. The position of K_c might be wrong compared to the two-dimensional Ising model ($K_c = 0.4407$), but the behaviour of the correlation length, which can be described by critical exponent ν_{Ising} obtained from the expression below remains unchanged,

$$b^{\frac{1}{\nu_{Ising}}} = \left. \frac{\partial K'}{\partial K} \right|_{K_c}. \quad (47)$$

The wrong K_c values can be attributed due to arbitrary $\{k_i\}$ values taken in $R(\sigma_1', \sigma_2')$ for easy evaluation. However, using the above expression, we can obtain $\nu_{Ising} = 1.019$ for $d = 2$, which is comparable with the exact value $\nu_{Ising} = 1$ [53]. We also obtain that as $d \rightarrow \infty$, $\nu_{Ising} \rightarrow 1$ for $a = 2$ which seems to be the typical behaviour of Migdall-Kadanoff bond moving approximation on d -dimensional hypercubic lattice [51]. We numerically deduce the strength of the long-range interactions $a \propto d$ dimensionality of the Ising model for describing the phase transitions on fractal systems. For $1 < d < 2$, we derive the empirical relation $a \sim 0.9d^{1.082}$, which can predict the behaviour of the correlation length at a critical point similar to that of the previous studies of Padé-Borel summation on Callan-Symanzik scheme of renormalization [58]. Using this relation, we compute ν_{Ising} for non-integer dimensions and compare it with literature in Table I.

III. CRITICAL EXPONENTS OF QUANTUM PHASE TRANSITIONS (GROSS-NEVEU-YUKAWA MODELS)

Recently Dirac materials [59] and Weyl semimetals [60] have been interesting to study since they are believed to undergo second-order quantum phase transitions under particular scenarios. Such transitions are experimentally yet to

TABLE I: Critical exponent of $O(1)$ class ν_{Ising} for $1 < d < 2$.

d	1.25	1.375	1.5	1.650	1.750	1.875
ν_{Ising}	2.9879	1.9414	1.5542	1.3162	1.2158	1.1253
ν_{Ising} [58]	2.593	1.983	1.627	1.353	1.223	1.098

be verified; however, their realization is theorised and studied with relevant order parameters related to the systems [61–68]. However, since quantum phase transitions can happen at $T = 0$, reduced temperature $|T - T_c|$ in the field-theoretic description is replaced with similar measures, such as variation of coupling constant from their critical values. While purely bosonic field theories describe $O(n)$ universality classes, a new class of universality emerges for Dirac and Weyl systems in the presence of fermionic fields described by Gross-Neveu-Yukawa (GNY) models [69, 70]. Recently four-loop RG functions have been solved for different GNY models to address the critical exponents of such universality classes [36]. However, they employed only simple diagonal Padé approximants to evaluate the critical exponents as spurious poles riddled the other non-diagonal terms. Typically a thorough analysis is required when using Padé-based methods with critical inspection for poles and their removal, as performed for different ϵ -expansions in recent work [21]. We use the four-loop ϵ expansions [36] to determine critical exponents related to these models implementing continued functions.

A. Chiral Ising universality class

The Chiral Ising model that can describe quantum phase transitions is a modification of the field-theoretic Ising model where fermions (ψ) are coupled to a scalar field (ϕ) with Yukawa coupling. There are additional critical exponents in these GNY models associated with the RG gamma functions of the real scalar field and fermions, anomalous dimensions of bosons (η_ϕ) and fermions (η_ψ). The difference in the description of such GNY models has been generalized by a parameter N , the number of fermion flavours of the four-component Dirac fermion in the model. These models have a range of applicability depending on N . The most physically relevant systems are the semimetal-charge density wave transition of electrons in graphene for $N = 2$ [71] and semimetal-insulator transition of spinless fermions on honeycomb lattice for $N = 1$. These systems have also been studied using other methods such as non-perturbative functional renormalization group (FRG) [72, 73], quantum Monte-Carlo simulations (QMC) [74–76] and CB [77, 78] to calculate their corresponding critical exponents. For $N = 1/4$, this model is theorised to exhibit emergent supersymmetry properties on the boundary of topological superconductors [79].

We implement continued exponential fraction, continued exponential and continued exponential with Borel-Leroy transformation (Eq.s (2), (3) and (4)) to obtain estimates for exponents [36]

$$1/\nu = 2 - 0.9524\epsilon + 0.007225\epsilon^2 - 0.09487\epsilon^3 - 0.01265\epsilon^4 \quad (48a)$$

$$\eta_\phi = 0.5714\epsilon + 0.1236\epsilon^2 - 0.02789\epsilon^3 + 0.1491\epsilon^4, \quad (48b)$$

$$\eta_\psi = 0.07143\epsilon - 0.006708\epsilon^2 - 0.02434\epsilon^3 + 0.01758\epsilon^4, \quad (48c)$$

$$\omega = \epsilon - 0.3525\epsilon^2 + 0.4857\epsilon^3 - 1.338\epsilon^4, \quad (48d)$$

for $N = 2$ in $d = 2 + 1$. These estimates at consecutive orders for $1/\nu$, η_ϕ , η_ψ and ω are illustrated, compared with QMC predictions [74] in Figs 11(a), 11(b), 12(a) and 12(b), respectively.

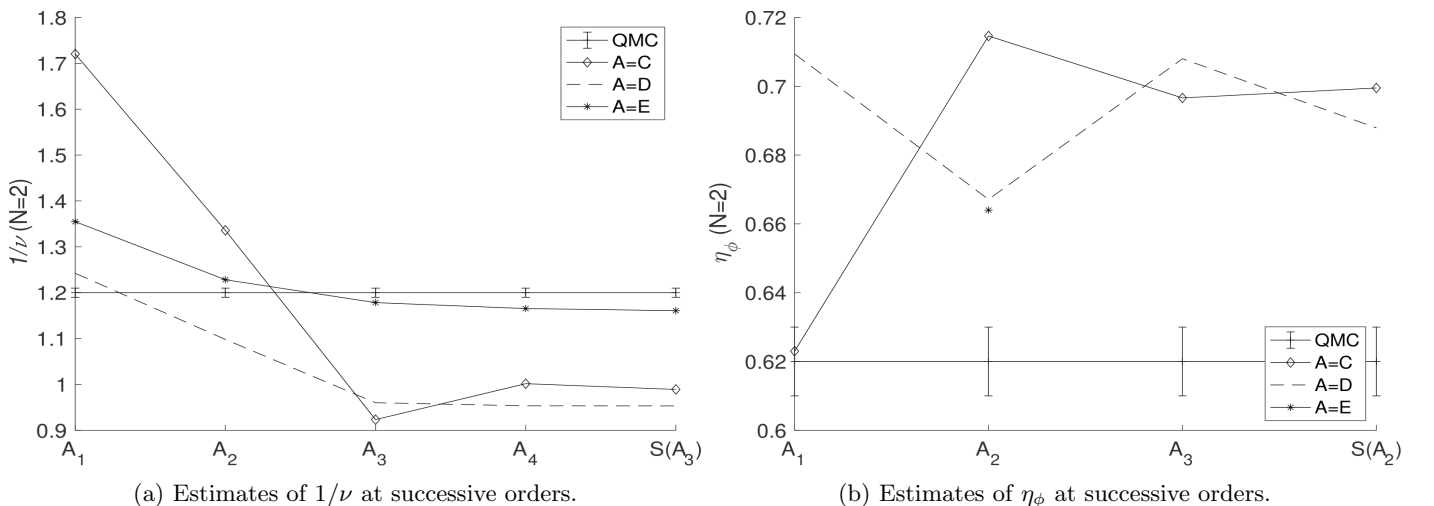


FIG. 11: Comparing Chiral Ising universality class $1/\nu$ and η_ϕ of $N = 2$ with QMC results [74].

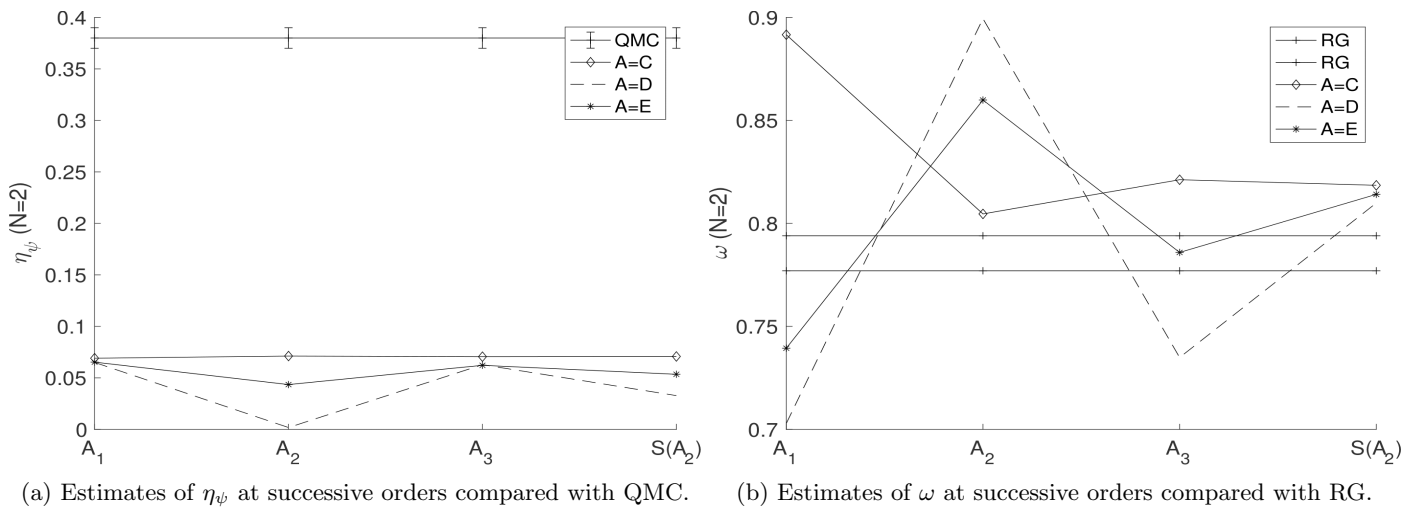


FIG. 12: Comparing Chiral Ising universality class η_ψ and ω of $N = 2$ with QMC [74] and RG [36] estimates.

Similarly, we obtain estimates for exponents [36]

$$1/\nu = 2 - 0.8347\epsilon - 0.0057\epsilon^2 - 0.0603\epsilon^3 - 0.0903\epsilon^4, \quad (49a)$$

$$\eta_\phi = 0.4\epsilon + 0.1025\epsilon^2 - 0.0632\epsilon^3 + 0.1986\epsilon^4, \quad (49b)$$

$$\eta_\psi = 0.1\epsilon - 0.0102\epsilon^2 - 0.0330\epsilon^3 + 0.0507\epsilon^4, \quad (49c)$$

for $N = 1$ in $d = 2 + 1$. These estimates at consecutive orders for $1/\nu$, η_ϕ and η_ψ are illustrated, compared with predictions from QMC [75, 76], CB [78] predictions in Figs. 13(a), 13(b) and 14(a), respectively.

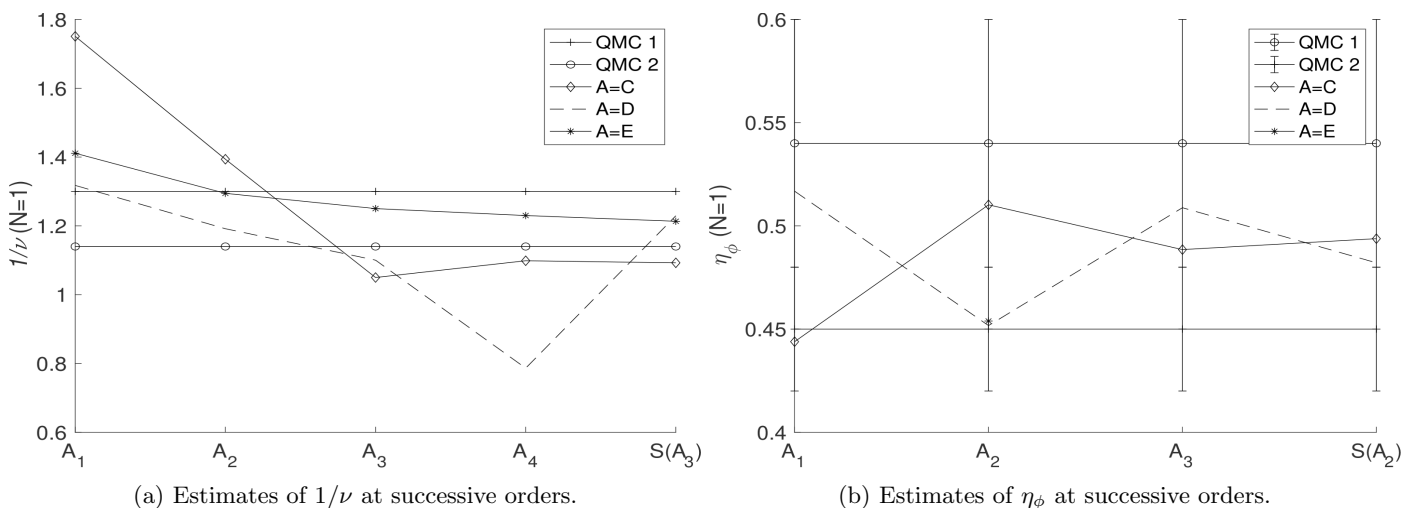


FIG. 13: Comparing Chiral Ising universality class $1/\nu$ and η_ϕ of $N = 1$ with QMC [75, 76] estimates.

And, similarly we obtain estimates for exponents [36]

$$1/\nu = 2 - 0.5714\epsilon - 0.0204\epsilon^2 + 0.0240\epsilon^3 - 0.0596\epsilon^4, \quad (50a)$$

$$\eta_\phi = \eta_\psi = 0.1429\epsilon + 0.0408\epsilon^2 - 0.0480\epsilon^3 + 0.1193\epsilon^4, \quad (50b)$$

$$\omega = \epsilon - 0.4286\epsilon^2 + 1.1763\epsilon^3 - 4.0099\epsilon^4, \quad (50c)$$

for $N = 1/4$ in $d = 2 + 1$ which are illustrated, compared with FRG predictions [80] in Figs. 15(a), 14(b), 15(b), respectively. We observe that these predictions tabulated in Table II are mostly comparable with existing literature from FRG, QMC, and CB and are precisely compatible with Padé resummation of RG [36]. Estimates seem to undershoot or overshoot slightly, whereas there is large uncertainty in predicting anomalous fermion dimension η_ψ for $N = 2, 1$ from different approaches. When handling η_ϕ, η_ψ with continued exponential with Borel-Leroy transformation, spurious poles were encountered, where estimates are not available.

B. Chiral XY universality class

In the chiral XY model, Dirac fermions undergo continuous $U(1)$ symmetry breaking described by a complex scalar field. The physically interesting systems in this model which can describe the quantum criticality of superconducting

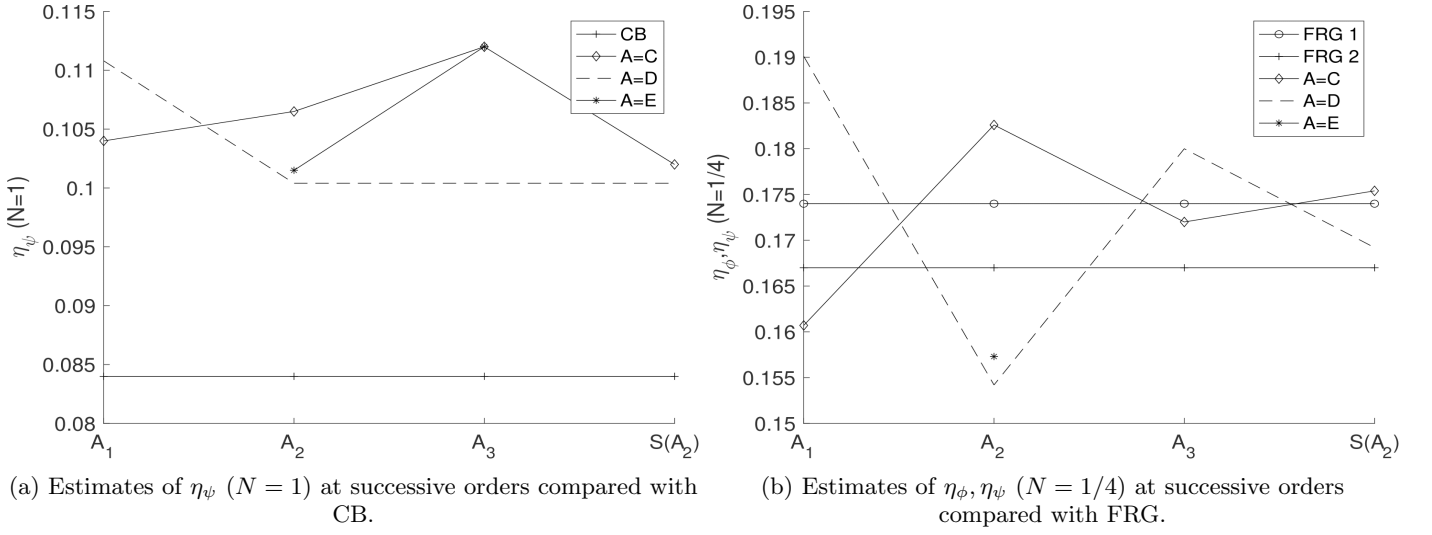


FIG. 14: Comparing Chiral Ising universality class η_ψ of $N=1, 1/4$ and η_ϕ of $N=1/4$ with CB [78] and FRG [80] estimates.

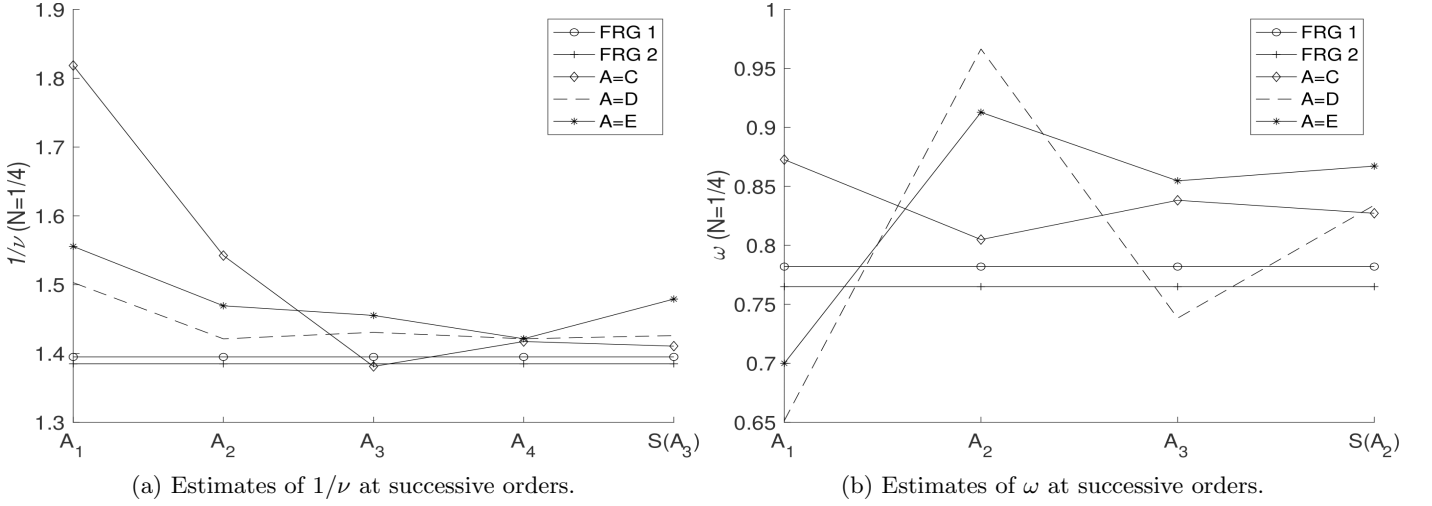


FIG. 15: Comparing Chiral Ising universality class $1/\nu$ and ω of $N=1/4$ with FRG [80] estimates.

TABLE II: Critical exponents of Chiral Ising universality class $1/\nu$, η_ϕ , η_ψ and ω for $N=2, 1, 1/4$. Our values derived from continued functions ($\{C, D, E\}$) are compared with recent literature.

N	$1/\nu$	η_ϕ	η_ψ	ω
2	0.989(45) ($S(C_3)$)	0.699(11) ($S(C_2)$)	0.0708 ($S(C_2)$)	0.8185(96) ($S(C_2)$) 0.81(12) ($S(D_2)$) 0.814(51) ($S(E_2)$) 0.794, 0.777 [36]
	0.9531(35) ($S(D_3)$)	0.688(31) ($S(D_2)$)	0.033(46) ($S(D_2)$)	
	1.1608(88) ($S(E_3)$)	0.664 (E_2)	0.054(14) ($S(E_2)$)	
	0.931, 0.945 [36]	0.7079, 0.6906 [36]	0.0539, 0.0506 [36]	
	0.994(2) [72] (FRG)	0.742 [78] (CB)	0.044 [78] (CB)	
	1.20(1) [74] (QMC)	0.7765 [72] (FRG)	0.0276 [72] (FRG)	
		0.62(1) [74] (QMC)	0.38(1) [74] (QMC)	
1	1.093(27) ($S(C_3)$)	0.494(14) ($S(C_2)$)	0.1019(77) ($S(C_2)$)	-
	1.23(38) ($S(D_3)$)	0.482(42) ($S(D_2)$)	0.1004 ($S(D_2)$)	
	1.213(18) ($S(E_3)$)	0.4539 (E_2)	0.1011 (E_3)	
	1.101 [36]	0.4969, 0.4872 [36]	0.0976, 0.0972 [36]	
	1.075(4) [72] (FRG)	0.5506 [72] (FRG)	0.0645 [72] (FRG)	
	1.14 [75] (QMC)	0.544 [78] (CB)	0.084 [78] (CB)	
	1.30 [76] (QMC)	0.54(6) [75] (QMC)		
	0.45(3)[76] (QMC)			
1/4	1.411(21) ($S(C_3)$)	0.1754(71) ($S(C_2)$)	0.1754(71) ($S(C_2)$)	0.827(22) ($S(C_2)$) 0.83(16) ($S(D_2)$) 0.867(35) ($S(E_2)$) 0.843, 0.838 [36] 0.765, 0.782 [80] (FRG)
	1.426(7) ($S(D_3)$)	0.169(18) ($S(D_2)$)	0.169(18) ($S(D_2)$)	
	1.479(46) ($S(E_3)$)	0.1573 (E_2)	0.1573 (E_2)	
	1.415 [36]	0.171, 0.170 [36]	0.171, 0.170 [36]	
	1.385, 1.395 [80] (FRG)	0.167, 0.174 [80] (FRG)	0.167, 0.174 [80] (FRG)	
		0.164[77] (CB)	0.164[77] (CB)	

states in graphene are for $N = 2$ [81]. This is related to Kekulé transition on two-dimensional graphene structures [82–84]. Another interesting application of this model is in surface states of three-dimensional topological insulators where emergent supersymmetry is theorised for $N = 1/2$ [81, 85]. We obtain the estimates of critical exponents [36]

$$1/\nu = 2 - 1.2\epsilon + 0.1829\epsilon^2 - 0.3515\epsilon^3 + 0.5164\epsilon^4, \quad (51a)$$

$$\eta_\phi = 0.6667\epsilon + 0.1211\epsilon^2 - 0.005048\epsilon^3 + 0.1938\epsilon^4, \quad (51b)$$

$$\eta_\psi = 0.1667\epsilon - 0.02722\epsilon^2 - 0.05507\epsilon^3 + 0.04202\epsilon^4, \quad (51c)$$

$$\omega = \epsilon - 0.3783\epsilon + 0.6271\epsilon^3 - 1.853\epsilon^4, \quad (51d)$$

for $N = 2$ in $d = 2 + 1$. These estimates at consecutive orders for $1/\nu$, η_ϕ , η_ψ and ω are illustrated, compared with predictions from QMC [86], FRG [87] in Figs 16(a), 16(b), 17(a) and 17(b), respectively. We obtain the estimates of

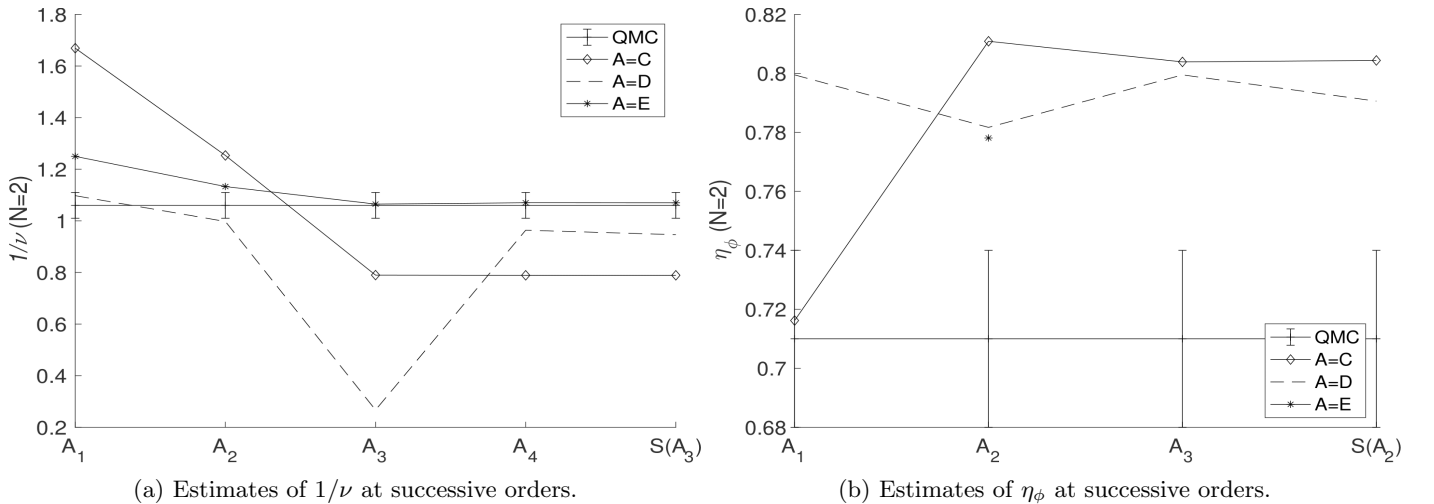


FIG. 16: Comparing Chiral XY universality class $1/\nu$ and η_ϕ of $N = 2$ with QMC [86] estimates.

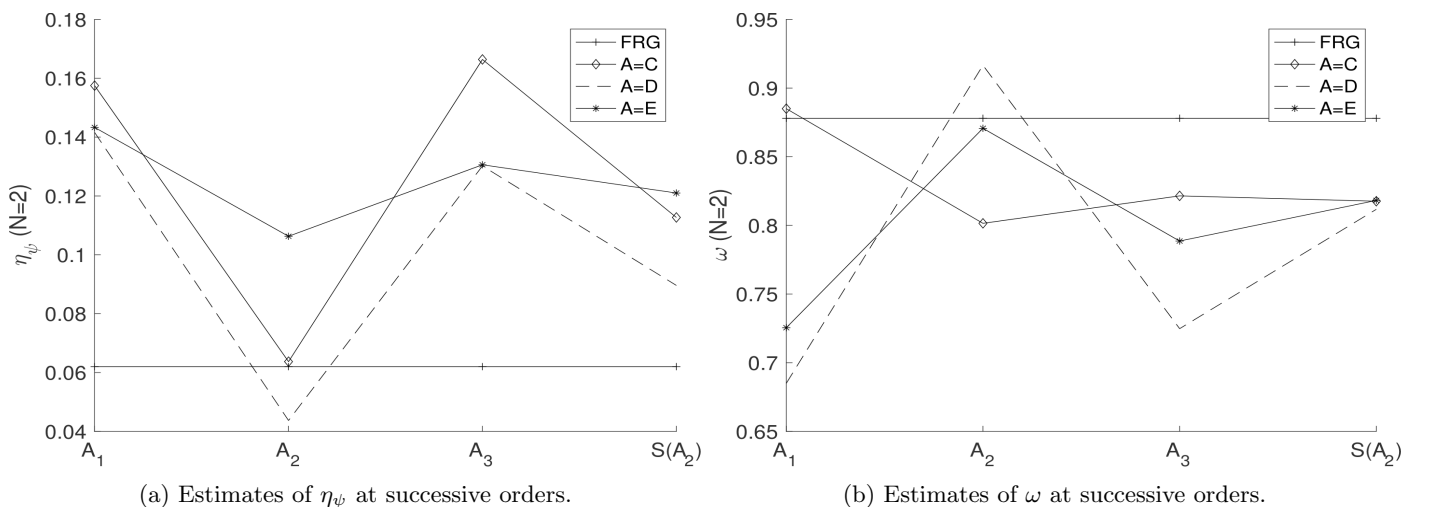


FIG. 17: Comparing Chiral XY universality class η_ψ and ω of $N = 2$ with FRG [87] estimates.

critical exponents [36]

$$1/\nu = 2 - \epsilon + 0.3333\epsilon^2 - 0.8569\epsilon^3 + 2.7629\epsilon^4, \quad (52a)$$

$$\eta_\phi = \eta_\psi = \epsilon/3, \quad (52b)$$

$$\omega = \epsilon - 0.3333\epsilon + 0.8569\epsilon^3 - 2.7629\epsilon^4, \quad (52c)$$

for $N = 1/2$ in $d = 2 + 1$. Estimates for $1/\nu$ and ω are illustrated, compared with predictions from CB [88] in Figs 18(a) and 18(b), respectively. The estimated values in Table III are comparable with predictions from other interesting field-theoretic studies of FRG [87], QMC [86], CB [88] and is compatible with Padé resummation [36].

C. Chiral Heisenberg universality class

In Chiral Heisenberg model $SU(2)$ symmetry is broken where the description of eight component spinors ($N = 2$) can correspond to transition towards an antiferromagnetic spin-density wave state in graphene and related materials [89–91].

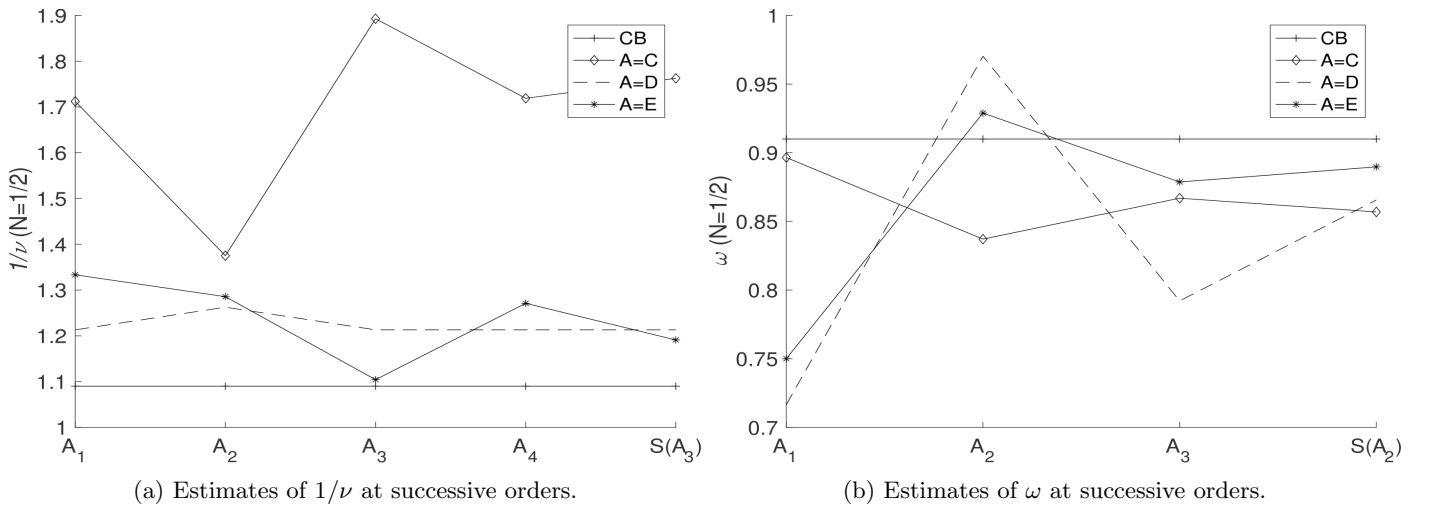


FIG. 18: Comparing Chiral XY universality class $1/\nu$ and ω of $N = 1/2$ with CB [88] estimates.

TABLE III: Critical exponents of Chiral XY universality class $1/\nu$, η_ϕ , η_ψ and ω for $N = 2, 1/4$. Our values are compared with recent literature.

N	$1/\nu$	η_ϕ	η_ψ	ω
2	0.7890 ($S(C_3)$)	0.8044(37) ($S(C_2)$)	0.113(78) ($S(C_2)$)	0.818(12) ($S(C_2)$)
	0.946(26) ($S(D_3)$)	0.791(13) ($S(D_2)$)	0.121(10) ($S(D_2)$)	0.81(14) ($S(D_2)$)
	1.0699(28) ($S(E_3)$)	0.7781 (E_2)	0.121(17) ($S(E_2)$)	0.818(56) ($S(E_2)$)
	0.840, 0.841 [36]	0.7079, 0.6906 [36]	0.117, 0.108 [36]	0.796, 0.780 [36]
	0.862 [87] (FRG)	0.88 [87] (FRG)	0.062 [87] (FRG)	0.878 [87] (FRG)
	1.06(5) [86] (QMC)	0.71(3) [86] (QMC)		
1/2	1.76(11) ($S(C_3)$)			0.857(20) ($S(C_2)$)
	1.237(37) ($S(D_3)$)	1/3	1/3	0.86(13) ($S(D_2)$)
	1.19(12) ($S(E_3)$)	1/3 [36]	1/3 [36]	0.890(31) ($S(E_2)$)
	1.128, 1.130 [36]	1/3 [88] (CB)	1/3 [88] (CB)	0.872, 0.870 [36]
	1.090 [88] (CB)			0.910 [88] (CB)

In this case, it is interesting to note that our precise estimates of critical exponents [36]

$$1/\nu = 2 - 1.527\epsilon + 0.4076\epsilon^2 - 0.8144\epsilon^3 + 2.001\epsilon^4, \quad (53a)$$

$$\eta_\phi = 0.8\epsilon + 0.1593\epsilon^2 + 0.02381\epsilon^3 + 0.2103\epsilon^4, \quad (53b)$$

$$\eta_\psi = 0.3\epsilon - 0.05760\epsilon^2 - 0.1184\epsilon^3 + 0.04388\epsilon^4, \quad (53c)$$

$$\omega = \epsilon - 0.4830\epsilon^2 + 0.9863\epsilon^3 - 2.627\epsilon^4, \quad (53d)$$

for $N = 2$ in $d = 2+1$ are more in comparison with previous predictions from FRG [92] and QMC [93, 94] than the simple Padé estimates [36] (Table IV). These estimates at consecutive orders for $1/\nu$, η_ϕ , η_ψ and ω are illustrated, compared with predictions from QMC [93, 94] in Figs 19(a), 19(b), 20(a) and 20(b), respectively.

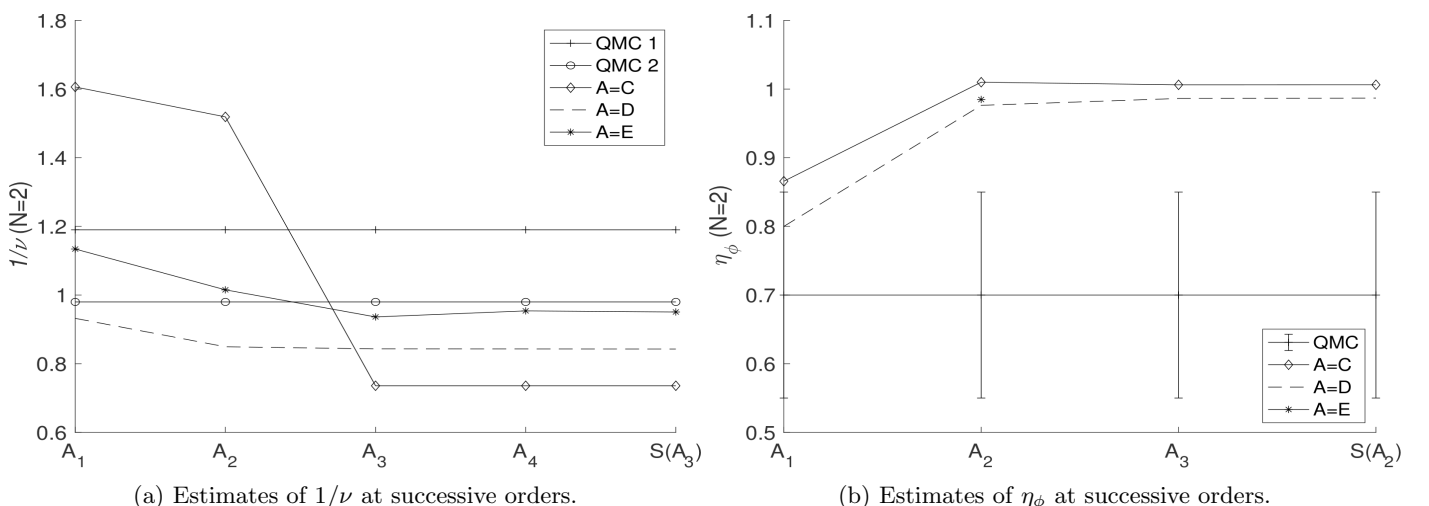


FIG. 19: Comparing Chiral Heisenberg universality class $1/\nu$ and η_ϕ of $N = 2$ with QMC [93, 94] estimates.

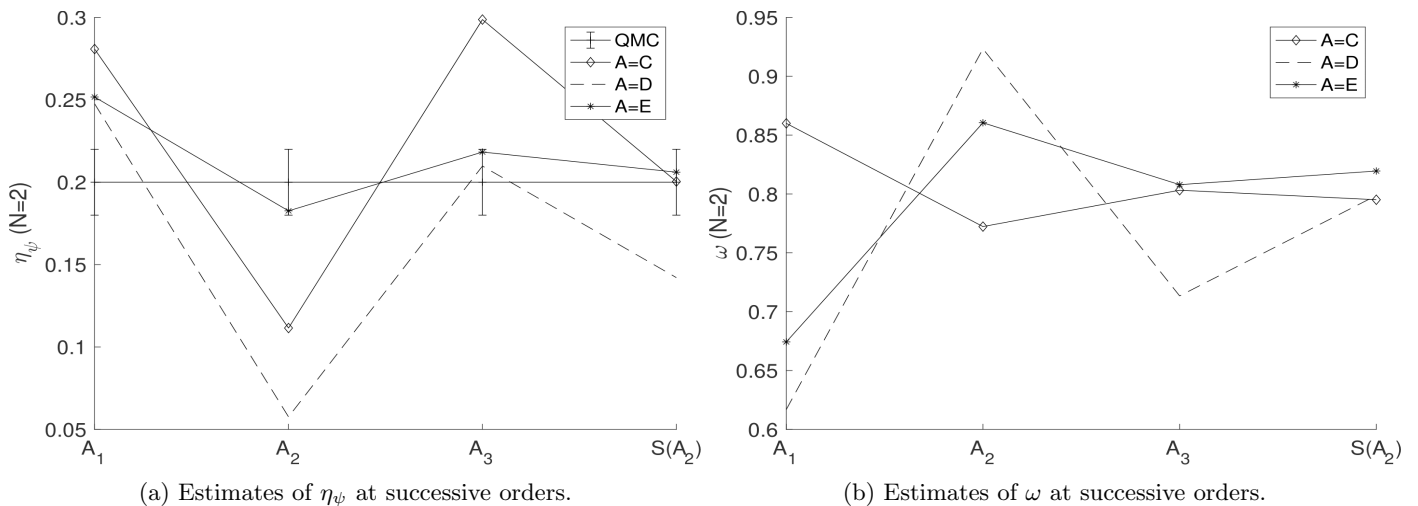


FIG. 20: Comparing Chiral Heisenberg universality class η_ψ and ω of $N = 2$ with QMC [94] estimates.

TABLE IV: Critical exponents of Chiral Heisenberg universality class $1/\nu$, η_ϕ , η_ψ and ω for $N = 2$. Our values compared with recent literature.

N	$1/\nu$	η_ϕ	η_ψ	ω
2	0.7358 ($S(C_3)$)	1.0063(19) ($S(C_2)$)	0.20(14) ($S(C_2)$)	
	0.8427(33) ($S(D_3)$)	0.9868(53) ($S(D_2)$)	0.14(11) ($S(D_2)$)	0.795(20) ($S(C_2)$)
	0.951(10) ($S(E_3)$)	0.9848 (E_2)	0.206(24) ($S(E_2)$)	0.79(15) ($S(D_2)$)
	0.6426, 0.6447 [36]	0.9985, 0.9563 [36]	0.1833, 0.1560 [36]	0.820(32) ($S(E_2)$)
	0.795 [92] (FRG)	1.032 [92] (FRG)	0.071 [92] (FRG)	
	0.98 [94] (QMC)	0.70(15) [93] (QMC)	0.20(2) [94] (QMC)	
	1.19 [93] (QMC)			

IV. CONCLUSION

Simple techniques were implemented on RG perturbative expansions of $O(n)$ -symmetric models and Gross-Neveu-Yukawa models to better define the nature of classical and quantum phase transitions. Precise critical parameters were derived in such systems from methods using continued functions. Only the first few terms in the perturbation series are used, and methods are tried without using arbitrarily free parameters which influence the convergence. Continued exponential was implemented on perturbative low-temperature expansions and position-space renormalization scheme of the Ising model to calculate critical exponents corresponding to the system.

One can further implement this convergence behaviour of continued functions on any wide range of perturbation methods to improve the convergence, especially when only a few terms are available in the divergent series. However, the accuracy of values we obtain from continued functions is only for small perturbation parameters, especially $\epsilon = 1$, which makes it an ideal method to study classical systems with 3 dimensions and quantum systems with 2+1 dimensions. Further, to improve it for larger perturbation parameters, one can try to use these continued functions to interpolate from both weak and strong coupling limits using the large-order asymptotic behaviour of the perturbation coefficients, if available. The exact and unique convergent properties of an individual continued function can be further studied more rigorously based on its limits of applicability and accuracy.

-
- [1] F. J. Dyson, “Divergence of perturbation theory in quantum electrodynamics,” *Phys. Rev.*, vol. 85, pp. 631–632, 1952.
- [2] E. Caliceti, M. Meyer-Hermann, P. Ribeca, A. Surzhykov, and U. Jentschura, “From useful algorithms for slowly convergent series to physical predictions based on divergent perturbative expansions,” *Physics Reports*, vol. 446, no. 1, pp. 1–96, 2007.
- [3] H. Kleinert and V. Schulte-Frohlinde, *Critical Properties of ϕ^4 -Theories*. WORLD SCIENTIFIC, 2001.
- [4] C. Bender and S. Orszag, *Advanced Mathematical Methods for Scientists and Engineers I: Asymptotic Methods and Perturbation Theory*. Advanced Mathematical Methods for Scientists and Engineers, Springer, 1999.
- [5] G. A. Baker, *Essentials of Padé approximants*. New York Academic Press, 1975.
- [6] G. A. Baker and P. Graves-Morris, *Padé Approximants*. Encyclopedia of Mathematics and its Applications, Cambridge University Press, 2 ed., 1996.
- [7] V. Abhignan and R. Sankaranarayanan, “Continued functions and perturbation series: Simple tools for convergence of diverging series in $O(n)$ -symmetric ϕ^4 field theory at weak coupling limit,” *Journal of Statistical Physics*, vol. 183, no. 1, p. 4, 2021.
- [8] C. M. Bender and J. P. Vinson, “Summation of power series by continued exponentials,” *Journal of Mathematical Physics*, vol. 37, no. 8, pp. 4103–4119, 1996.
- [9] M. Campostrini, M. Hasenbusch, A. Pelissetto, and E. Vicari, “Theoretical estimates of the critical exponents of the superfluid transition in ^4He by lattice methods,” *Phys. Rev. B*, vol. 74, p. 144506, 2006.

- [10] S. M. Chester, W. Landry, J. Liu, D. Poland, D. Simmons-Duffin, N. Su, and A. Vichi, “Carving out open space and precise $O(2)$ model critical exponents,” *Journal of High Energy Physics*, vol. 2020, no. 6, p. 142, 2020.
- [11] G. De Polsi, I. Balog, M. Tissier, and N. Wschebor, “Precision calculation of critical exponents in the $O(N)$ universality classes with the nonperturbative renormalization group,” *Phys. Rev. E*, vol. 101, p. 042113, 2020.
- [12] M. Hasenbusch, “Monte carlo study of an improved clock model in three dimensions,” *Phys. Rev. B*, vol. 100, p. 224517, Dec 2019.
- [13] J. A. Lipa, J. A. Nissen, D. A. Stricker, D. R. Swanson, and T. C. P. Chui, “Specific heat of liquid helium in zero gravity very near the lambda point,” *Phys. Rev. B*, vol. 68, p. 174518, 2003.
- [14] A. M. Shalaby, “ λ -point anomaly in view of the seven-loop hypergeometric resummation for the critical exponent ν of the $O(2)$ ϕ^4 model,” *Phys. Rev. D*, vol. 102, p. 105017, 2020.
- [15] A. M. Shalaby, “Critical exponents of the $O(N)$ -symmetric ϕ^4 model from the ϵ^7 hypergeometric-meijer resummation,” *The European Physical Journal C*, 2021.
- [16] O. Schnetz, “Numbers and functions in quantum field theory,” *Phys. Rev. D*, vol. 97, p. 085018, 2018.
- [17] M. Hasenbusch, “Finite size scaling study of lattice models in the three-dimensional Ising universality class,” *Phys. Rev. B*, vol. 82, p. 174433, 2010.
- [18] F. Kos, D. Poland, D. Simmons-Duffin, and A. Vichi, “Precision islands in the Ising and $O(n)$ models,” *Journal of High Energy Physics*, vol. 2016, no. 8, p. 36, 2016.
- [19] V. Abhignan and R. Sankaranarayanan, “Continued functions and Borel-Leroy transformation: Resummation of six-loop ϵ -expansions from different universality classes,” *Journal of Physics A: Mathematical and Theoretical*, 2021.
- [20] L. T. Adzhemyan, E. V. Ivanova, M. V. Kompaniets, A. Kudlis, and A. I. Sokolov, “Six-loop ϵ expansion study of three-dimensional n -vector model with cubic anisotropy,” *Nuclear Physics B*, vol. 940, pp. 332 – 350, 2019.
- [21] M. Kompaniets, A. Kudlis, and A. Sokolov, “Six-loop ϵ expansion study of three-dimensional $O(n) \times O(m)$ spin models,” *Nuclear Physics B*, vol. 950, p. 114874, 2020.
- [22] M. V. Kompaniets, A. Kudlis, and A. I. Sokolov, “Critical behavior of the weakly disordered Ising model: Six-loop $\sqrt{\epsilon}$ expansion study,” *Phys. Rev. E*, vol. 103, p. 022134, 2021.
- [23] V. I. Yukalov, “Interplay between approximation theory and renormalization group,” *Physics of Particles and Nuclei*, vol. 50, no. 2, pp. 141–209, 2019.
- [24] V. I. Yukalov and E. P. Yukalova, “From asymptotic series to self-similar approximants,” *Physics*, vol. 3, no. 4, pp. 829–878, 2021.
- [25] H. Mera, T. G. Pedersen, and B. K. Nikolić, “Nonperturbative quantum physics from low-order perturbation theory,” *Phys. Rev. Lett.*, vol. 115, p. 143001, 2015.
- [26] H. Mera, T. G. Pedersen, and B. K. Nikolić, “Fast summation of divergent series and resurgent transseries from meijer- g approximants,” *Phys. Rev. D*, vol. 97, p. 105027, 2018.
- [27] A. M. Shalaby, “Weak-coupling, strong-coupling and large-order parametrization of the hypergeometric-meijer approximants,” *Results in Physics*, vol. 19, p. 103376, 2020.
- [28] E. B. V. Vleck, “On the convergence of the continued fraction of Gauss and other continued fractions,” *Annals of Mathematics*, vol. 3, no. 1/4, pp. 1–18, 1901.
- [29] M. V. Kompaniets and E. Panzer, “Minimally subtracted six-loop renormalization of $O(n)$ -symmetric ϕ^4 theory and critical exponents,” *Phys. Rev. D*, vol. 96, p. 036016, 2017.
- [30] A. I. Aptekarev, V. I. Buslaev, A. Martinez-Finkelshtein, and S. P. Suetin, “Padé approximants, continued fractions, and orthogonal polynomials,” *Russian Mathematical Surveys*, vol. 66, no. 6, pp. 1049–1131, 2011.
- [31] A. Bultheel, P. Gonzalez-Vera, E. Hendriksen, and O. Njaastad, *Orthogonal Rational Functions and Continued Fractions*. Springer Netherlands, 2001.
- [32] L. Lorentzen, “Padé approximation and continued fractions,” *Applied Numerical Mathematics*, vol. 60, no. 12, pp. 1364 – 1370, 2010. Approximation and extrapolation of convergent and divergent sequences and series (CIRM, Luminy - France, 2009).
- [33] E. Ising, “Beitrag zur Theorie des Ferromagnetismus,” *Zeitschrift für Physik*, vol. 31, no. 1, pp. 253–258, 1925.
- [34] C. Domb, “On the theory of cooperative phenomena in crystals,” *Advances in Physics*, vol. 9, no. 34, pp. 149–244, 1960.
- [35] L. P. Kadanoff, “Notes on Migdal’s Recursion Formulas,” *Annals Phys.*, vol. 100, pp. 359–394, 1976.
- [36] N. Zerf, L. N. Mihaila, P. Marquard, I. F. Herbut, and M. M. Scherer, “Four-loop critical exponents for the Gross-Neveu-Yukawa models,” *Phys. Rev. D*, vol. 96, p. 096010, 2017.
- [37] L. D. Landau, “On the theory of phase transitions,” *Zh. Eksp. Teor. Fiz.*, vol. 7, pp. 19–32, 1937. [Ukr. J. Phys.53,25(2008)].
- [38] L. P. Kadanoff, W. Gotze, D. Hamblen, R. Hecht, E. A. S. Lewis, V. V. Palciauskas, M. Rayl, J. Swift, D. Aspnes, and J. Kane, “Static Phenomena Near Critical Points: Theory and Experiment,” *Rev. Mod. Phys.*, vol. 39, pp. 395–431, 1967.
- [39] K. G. Wilson and J. B. Kogut, “The Renormalization group and the epsilon expansion,” *Phys. Rept.*, vol. 12, pp. 75–199, 1974.
- [40] D. Poland, “Summation of series in statistical mechanics by continued exponentials,” *Physica A: Statistical Mechanics and its Applications*, vol. 250, no. 1, pp. 394 – 422, 1998.
- [41] B. Delamotte, M. Dudka, Y. Holovatch, and D. Mouhanna, “Relevance of the fixed dimension perturbative approach to frustrated magnets in two and three dimensions,” *Phys. Rev. B*, vol. 82, p. 104432, Sep 2010.
- [42] N. Clisby and B. Dünweg, “High-precision estimate of the hydrodynamic radius for self-avoiding walks,” *Phys. Rev. E*, vol. 94, p. 052102, Nov 2016.
- [43] M. Kompaniets and K. J. Wiese, “Fractal dimension of critical curves in the $O(n)$ -symmetric ϕ^4 model and crossover exponent at 6-loop order: Loop-erased random walks, self-avoiding walks, Ising, XY , and Heisenberg models,” *Phys. Rev. E*, vol. 101, p. 012104, 2020.
- [44] A. C. Echeverri, B. von Harling, and M. Serone, “The effective bootstrap,” *Journal of High Energy Physics*, vol. 2016, no. 9, p. 97, 2016.
- [45] M. Hasenbusch, “Eliminating leading corrections to scaling in the three-dimensional $O(N)$ -symmetric ϕ^4 model: $N = 3$ and 4,” *Journal of Physics A: Mathematical and General*, vol. 34, no. 40, p. 8221, 2001.
- [46] J.-P. Eckmann, J. Magnen, and R. Sénéor, “Decay properties and Borel summability for the Schwinger functions in $P(\Phi)_2$ theories,” *Communications in Mathematical Physics*, vol. 39, no. 4, pp. 251–271, 1975.
- [47] E. V. Orlov and A. I. Sokolov, “Critical thermodynamics of two-dimensional systems in the five-loop renormalization-group approximation,” *Physics of the Solid State*, vol. 42, no. 11, pp. 2151–2158, 2000.

- [48] P. Calabrese, M. Caselle, A. Celi, A. Pelissetto, and E. Vicari, “Non-analyticity of the Callan-Symanzik β -function of two-dimensional $\mathbf{O}(n)$ models,” *Journal of Physics A: Mathematical and General*, vol. 33, no. 46, pp. 8155–8170, 2000.
- [49] B. Nienhuis, “Exact critical point and critical exponents of $\mathbf{O}(n)$ models in two dimensions,” *Phys. Rev. Lett.*, vol. 49, pp. 1062–1065, 1982.
- [50] S. Caracciolo, A. J. Guttmann, I. Jensen, A. Pelissetto, A. N. Rogers, and A. D. Sokal, “Correction-to-scaling exponents for two-dimensional self-avoiding walks,” *Journal of Statistical Physics*, vol. 120, no. 5, pp. 1037–1100, 2005.
- [51] M. Kardar, *Statistical Physics of Fields*. Cambridge University Press, 2007.
- [52] H. A. Kramers and G. H. Wannier, “Statistics of the two-dimensional ferromagnet. part I,” *Phys. Rev.*, vol. 60, pp. 252–262, 1941.
- [53] L. Onsager, “Crystal statistics. I. a two-dimensional model with an order-disorder transition,” *Phys. Rev.*, vol. 65, pp. 117–149, 1944.
- [54] G. A. Baker, “Further applications of the Padé approximant method to the Ising and Heisenberg models,” *Phys. Rev.*, vol. 129, pp. 99–102, 1963.
- [55] C. Domb, “Series expansions for ferromagnetic models,” *Advances in Physics*, vol. 19, no. 79, pp. 339–370, 1970.
- [56] G. Martinelli and G. Parisi, “A systematical improvement of the Migdal recursion formula,” *Nuclear Physics B*, vol. 180, no. 2, pp. 201 – 220, 1981.
- [57] S. Caracciolo, “Improved Migdal recursion formula for the Ising model in two dimensions on a triangular lattice,” *Nuclear Physics B*, vol. 180, no. 3, pp. 405 – 416, 1981.
- [58] Y. Holovatch, “Critical exponents of Ising-like systems in general dimensions,” *Theoretical and Mathematical Physics*, vol. 96, no. 3, pp. 1099–1109, 1993.
- [59] T. Wehling, A. Black-Schaffer, and A. Balatsky, “Dirac materials,” *Advances in Physics*, vol. 63, no. 1, pp. 1–76, 2014.
- [60] O. Vafek and A. Vishwanath, “Dirac fermions in solids: From high-Tc cuprates and graphene to topological insulators and Weyl semimetals,” *Annual Review of Condensed Matter Physics*, vol. 5, no. 1, pp. 83–112, 2014.
- [61] S. V. Syzranov, P. M. Ostrovsky, V. Gurarie, and L. Radzihovsky, “Critical exponents at the unconventional disorder-driven transition in a Weyl semimetal,” *Phys. Rev. B*, vol. 93, p. 155113, 2016.
- [62] T. Louvet, D. Carpentier, and A. A. Fedorenko, “On the disorder-driven quantum transition in three-dimensional relativistic metals,” *Phys. Rev. B*, vol. 94, p. 220201, 2016.
- [63] K. Kobayashi, T. Ohtsuki, K.-I. Imura, and I. F. Herbut, “Density of states scaling at the semimetal to metal transition in three dimensional topological insulators,” *Phys. Rev. Lett.*, vol. 112, p. 016402, 2014.
- [64] J. Maciejko and R. Nandkishore, “Weyl semimetals with short-range interactions,” *Phys. Rev. B*, vol. 90, p. 035126, 2014.
- [65] P. Goswami and S. Chakravarty, “Quantum criticality between topological and band insulators in $\mathbf{3} + \mathbf{1}$ dimensions,” *Phys. Rev. Lett.*, vol. 107, p. 196803, 2011.
- [66] D. V. Khveshchenko, “Ghost excitonic insulator transition in layered graphite,” *Phys. Rev. Lett.*, vol. 87, p. 246802, 2001.
- [67] I. F. Herbut, “Interactions and phase transitions on graphene’s honeycomb lattice,” *Phys. Rev. Lett.*, vol. 97, p. 146401, 2006.
- [68] C. Honerkamp, “Density waves and Cooper pairing on the honeycomb lattice,” *Phys. Rev. Lett.*, vol. 100, p. 146404, 2008.
- [69] J. Zinn-Justin, “Four-fermion interaction near four dimensions,” *Nuclear Physics B*, vol. 367, no. 1, pp. 105–122, 1991.
- [70] B. Rosenstein, Hoi-Lai Yu, and A. Kovner, “Critical exponents of new universality classes,” *Physics Letters B*, vol. 314, no. 3, pp. 381–386, 1993.
- [71] I. F. Herbut, “Interactions and phase transitions on graphene’s honeycomb lattice,” *Phys. Rev. Lett.*, vol. 97, p. 146401, 2006.
- [72] B. Knorr, “Ising and Gross-Neveu model in next-to-leading order,” *Phys. Rev. B*, vol. 94, p. 245102, 2016.
- [73] L. Janssen and I. F. Herbut, “Antiferromagnetic critical point on graphene’s honeycomb lattice: A functional renormalization group approach,” *Phys. Rev. B*, vol. 89, p. 205403, 2014.
- [74] S. Chandrasekharan and A. Li, “Quantum critical behavior in three dimensional lattice Gross-Neveu models,” *Phys. Rev. D*, vol. 88, p. 021701, 2013.
- [75] E. Huffman and S. Chandrasekharan, “Fermion bag approach to hamiltonian lattice field theories in continuous time,” *Phys. Rev. D*, vol. 96, p. 114502, 2017.
- [76] Z.-X. Li, Y.-F. Jiang, and H. Yao, “Fermion-sign-free Majorana-quantum-Monte-Carlo studies of quantum critical phenomena of Dirac fermions in two dimensions,” *New J. Phys.*, vol. 17, no. 8, p. 085003, 2015.
- [77] L. Iliesiu, F. Kos, D. Poland, S. S. Pufu, D. Simmons-Duffin, and R. Yacoby, “Fermion-scalar conformal blocks,” *Journal of High Energy Physics*, vol. 2016, no. 4, p. 74, 2016.
- [78] L. Iliesiu, F. Kos, D. Poland, S. S. Pufu, and D. Simmons-Duffin, “Bootstrapping 3d fermions with global symmetries,” *Journal of High Energy Physics*, vol. 2018, no. 1, p. 36, 2018.
- [79] T. Grover, D. N. Sheng, and A. Vishwanath, “Emergent space-time supersymmetry at the boundary of a topological phase,” *Science*, vol. 344, no. 6181, pp. 280–283, 2014.
- [80] H. Gies, T. Hellwig, A. Wipf, and O. Zanusso, “A functional perspective on emergent supersymmetry,” *Journal of High Energy Physics*, vol. 2017, no. 12, p. 132, 2017.
- [81] B. Roy, V. Juričić, and I. F. Herbut, “Quantum superconducting criticality in graphene and topological insulators,” *Phys. Rev. B*, vol. 87, p. 041401, 2013.
- [82] C.-Y. Hou, C. Chamon, and C. Mudry, “Electron fractionalization in two-dimensional graphenelike structures,” *Phys. Rev. Lett.*, vol. 98, p. 186809, 2007.
- [83] S. Ryu, C. Mudry, C.-Y. Hou, and C. Chamon, “Masses in graphenelike two-dimensional electronic systems: Topological defects in order parameters and their fractional exchange statistics,” *Phys. Rev. B*, vol. 80, p. 205319, 2009.
- [84] B. Roy and I. F. Herbut, “Unconventional superconductivity on honeycomb lattice: Theory of Kekule order parameter,” *Phys. Rev. B*, vol. 82, p. 035429, 2010.
- [85] S.-S. Lee, “Emergence of supersymmetry at a critical point of a lattice model,” *Phys. Rev. B*, vol. 76, p. 075103, 2007.
- [86] Z.-X. Li, Y.-F. Jiang, S.-K. Jian, and H. Yao, “Fermion-induced quantum critical points,” *Nature Communications*, vol. 8, no. 1, p. 314, 2017.
- [87] L. Classen, I. F. Herbut, and M. M. Scherer, “Fluctuation-induced continuous transition and quantum criticality in Dirac semimetals,” *Phys. Rev. B*, vol. 96, p. 115132, 2017.
- [88] N. Bobev, S. El-Showk, D. Mazáč, and M. F. Paulos, “Bootstrapping the three dimensional supersymmetric Ising model,” *Phys. Rev. Lett.*, vol. 115, p. 051601, 2015.
- [89] I. F. Herbut, “Interactions and phase transitions on graphene’s honeycomb lattice,” *Phys. Rev. Lett.*, vol. 97, p. 146401, 2006.
- [90] C. Honerkamp, “Density waves and cooper pairing on the honeycomb lattice,” *Phys. Rev. Lett.*, vol. 100, p. 146404, 2008.

- [91] M. V. Ulybyshev, P. V. Buividovich, M. I. Katsnelson, and M. I. Polikarpov, “Monte carlo study of the semimetal-insulator phase transition in monolayer graphene with a realistic interelectron interaction potential,” *Phys. Rev. Lett.*, vol. 111, p. 056801, 2013.
- [92] B. Knorr, “Critical chiral Heisenberg model with the functional renormalization group,” *Phys. Rev. B*, vol. 97, p. 075129, 2018.
- [93] F. Parisen Toldin, M. Hohenadler, F. F. Assaad, and I. F. Herbut, “Fermionic quantum criticality in honeycomb and π -flux hubbard models: Finite-size scaling of renormalization-group-invariant observables from quantum monte carlo,” *Phys. Rev. B*, vol. 91, p. 165108, 2015.
- [94] Y. Otsuka, S. Yunoki, and S. Sorella, “Universal quantum criticality in the metal-insulator transition of two-dimensional interacting Dirac electrons,” *Phys. Rev. X*, vol. 6, p. 011029, 2016.